Dinuclear Pyridine-4-thiolate-bridged Rhodium and Iridium Complexes as Ditopic Building Blocks in Molecular Architecture

Montserrat Ferrer,[*,a] Daniel Gómez-Bautista,[b] Albert Gutiérrez,[a] José R. Miranda,[b] Guillermo Orduña-Marco,[b] Luis A. Oro,[b] Jesús J. Pérez-Torrente,*[*,b] Oriol Rossell,[a] Pilar García-Orduña,[b] and Fernando J. Lahoz,[b]*

[a] Departament de Química Inorgànica, Universitat de Barcelona, c/ Martí i Franquès 1-11 08028 Barcelona, Spain.

[b] Departamento de Química Inorgánica, Instituto de Síntesis Química y Catálisis Homogénea–ISQCH, Universidad de Zaragoza–CSIC, Facultad de Ciencias, C/ Pedro Cerbuna, 12, 50009 Zaragoza, Spain.

Abstract

A series of dinuclear pyridine-4-thiolate rhodium and iridium compounds [M(μ-4-Spy)(diolef)]$_2$ (diolef = 1,5-cyclooctadiene, cod; M = Rh (**1**), Ir (**2**); 2,5-norbornadiene, nbd; M = Rh (**3**)) have been prepared by reaction of Li(4-Spy) with the appropriate compound [M(μ-Cl)(diolef)]$_2$ (M = Rh, Ir). The dinuclear compound [Rh(μ-4-Spy)(CO)(PPh$_3$)]$_2$ (**4**) has been obtained by reaction of [Rh(acac)(CO)(PPh$_3$] with 4-pySH. Compounds **1**-**4** have been assessed as metalloligands in self-assembly reactions with the *cis*-blocked [M(cod)(NCCH$_3$)$_2$](BF$_4$) (M = Rh (**a**) and M = Ir (**b**)) and [M(H$_2$O)$_2$(dppp)](OTf)$_2$ (M = Pd (**c**), Pt (**d**)) (dppp = 1,3-bis(diphenylphosphino)propane) acceptors. Homo [{M$_2$(μ-4-Spy)$_2$(cod)$_2$}$_2${M(cod)}$_2$](BF$_4$)$_2$ (M = Rh (**1a**)$_2$, and M = Ir (**2b**)$_2$), and hetero [{Rh$_2$(μ-4-Spy)$_2$(cod)$_2$}$_2${Ir(cod)}$_2$](BF$_4$)$_2$ (**1b**)$_2$, [{Rh$_2$(μ-4-Spy)$_2$(cod)$_2$}$_2${M'(dppp)}$_2$](OTf)$_4$ (M' = Pd (**1c**)$_2$ and M'= Pt (**1d**)$_2$) and [{Ir$_2$(μ-4-Spy)$_2$(cod)$_2$}$_2${M'(dppp)}$_2$](OTf)$_4$ (M' = Pd (**2c**)$_2$ and M'= Pt (**2d**)$_2$) hexanuclear metallomacrocycles have been obtained. NMR spectroscopy, in combination with ESI mass spectrometry has been used to elucidate the nature of the metalloligands and their respective supramolecular assemblies. Most of synthesized species have shown to be non-rigid in solution and their fluxional behavior has been studied by VT ^{1}H NMR spectroscopy. An X-ray diffraction study on the assemblies (**1a**)$_2$ and (**1d**)$_2$ revealed the formation of rectangular (9.6 x 6.6 Å) hexanuclear metallomacrocycles with alternating dinuclear (Rh$_2$) and mononuclear (Rh or Pt) corners. The hexanuclear core is supported by four pyridine-4-thiolate linkers, which are bonded through the thiolate moiety to the dinuclear rhodium units, exhibiting a bent-*anti* arrangement, and through the peripheral pyridinic nitrogen atoms to the mononuclear corners.

Introduction

The search for new and complex structures has been a motivating factor for the intensive study of metalla-supramolecular chemistry.[1-14] The sustained interest in this area is driven by the wide range of potential applications of these species in gas storage,[15,16] catalysis,[17-20] molecular magnetism,[21-23] optical materials,[24-26] sensoring[27-29] and many other areas.

In metal-based supramolecules, the metal units play an important role in controlling the structural geometries and tuning the chemical and physical properties of the compounds. In contrast with the synthesis of functionalized organic compounds, which can be achieved with high specificity by use of well-defined reactions and reagents, creation of complex metal-based molecules remains highly challenging because of the dynamic properties and lability of many coordination bonds. Although self-assembly has been proved to be a powerful tool to achieve a remarkable number of ordered structures,[11,12] such an approach depends largely on the availability of the metal-based building blocks suitable for the assembling.

Lately, we have become interested in the design and synthesis of heterometallic macrocyclic species[30-32] since the presence of different metal moieties can confer cooperative and/or dual behavior to the final species, particularly in that related with their participation in catalytic processes.[33-35] Although other methods have been described, the most common strategy to synthesize heterometallic macrocycles is the named modular self-assembly. This methodology requires the initial synthesis of metalloligands, i. e. coordination complexes with strong covalently bound ligands that have additional donor sites for coordination to further acceptor metallic building blocks.

In the general approach, monometallic building blocks are combined to yield self-assembled architectures. Despite the fact that the use of bimetallic units in combination with acceptor metallic complexes opens up new prospects for research in this area, only a handful number of bimetallic metalloligands have been described so far. In this context, Re_2,[36-38]

Co_2[39,40] and Mo_2[40,41] metal-metal bonded entities bearing either two terminal pyridine or phosphine groups have been successfully employed for this purpose (Chart 1). Interestingly, the anionic compound $[(C_6F_5)_2Pt(\mu\text{-}PPh_2)Pt(CN)_2]^{2-}$ described by Fornies et al.[42] is, to our knowledge, the unique example of a bimetallic building block lacking metal-metal bonds that coordinates to additional metal centers by terminal cyanide groups that are coordinated to one of the platinum atoms of the binuclear complex (Chart 1).

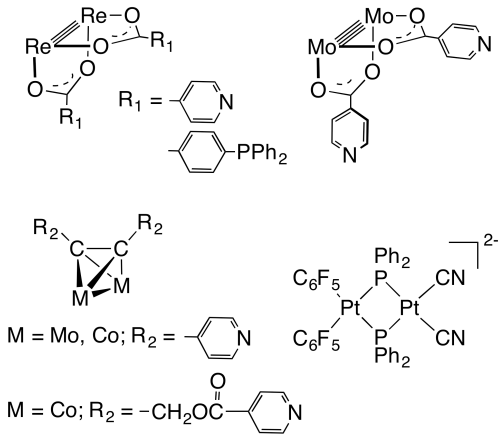

Chart 1. Schematic representation of reported bimetallic metalloligands.

In considering the goal of connecting dinuclear and mononuclear units, and given our experience in the synthesis and characterization of thiolate-bridged rhodium and iridium dinuclear complexes[43-47] and related hydrosulfide-bridged counterparts,[48] we envisaged the design of angular flexible dinuclear metalloligands of the type $[M(\mu\text{-}SR)L_2]_2$ (M = Rh, Ir) as precursors for new inorganic architectures by using adequately functionalized thiolato ligands. In this context, dinuclear d^8 transition-metal complexes with bridging thiolates have attracted widespread interest because of their electronic, structural and conformational properties,[45,49-55] and its catalytic activity in the hydroformylation of olefins under mild conditions.[56-60] Monodentate thiolato bridging ligands provided flexible structures that support a wide range of bonding and non-bonding metal distances by modification of the hinge angle

between the rhodium coordination planes. In addition, the existence of several conformers arising from the relative disposition of both thiolato ligands into the dinuclear framework and their possible interconversion, confers to the complexes an unusual versatility from the point of view of its potential application as syntons in supramolecular chemistry.

On the other hand, pyridine-4-thiol is a versatile ligand, since it has a potential coordinating ability to transition metals both through the sulfur or the nitrogen atoms. Moreover, the deprotonated pyridine-4-thiolato ligand usually coordinates to transition metals through the sulfur atom while leaving the pyridine moiety free. We thought that if the bimetallic complexes based on pyridine-4-thiolato ligands $[M(\mu\text{-}4\text{-}Spy)L_2]_2$ (M = Rh , Ir) could be prepared, the dangling pyridine groups would be available for further coordination to additional metal centers as the organometallic d^8-$[M(cod)(CH_3CN)_2]^+$ (M = Rh, Ir) or the dppp-chelated d^8-$[M(H_2O)_2(dppp)]^{2+}$ (M = Pd, Pt) metal fragments bearing labile acetonitrile and aqua ligands, respectively. Surprisingly, although the presence of uncoordinated pyridine groups strongly suggests the possibility of synthesizing novel supramolecular systems the number of reported discrete metallomacrocycles incorporating this ligand is relatively scarce. In this regard, the trinuclear $[Cp^*MCl(\mu\text{-}4\text{-}Spy)]_3$ (M = Ir,[61,62] Rh[62]) and $[PdCl(PPh_3)(\mu\text{-}4\text{-}Spy)]_3$,[63] the tetranuclear $[Cp^*Ir(4\text{-}Spy)(\mu\text{-}4\text{-}Spy)]_4$,[61] and the heterotetranuclear [Pt(4,4'-dtbpy)(μ-4-Spy)$(ZnCl_2)]_2$(dtbpy= 4,4'-di-tert-butyl-2,2'-bipyridine)[64] species are, to the best of our knowledge, the only reported examples.

In this paper, we report on the synthesis of dinuclear rhodium or iridium organometallic ditopic metalloligands bridged by pyridine-4-thiolato ligands and their successful application in the construction of rectangular hexanuclear homo and heterometallomacrocyles with alternating Rh_2 or Ir_2 and Rh, Ir, Pd or Pt corners.

Experimental Section

General Methods. All manipulations were performed under a dry argon or nitrogen atmosphere using Schlenk-tube techniques. Unless otherwise stated, all reactions were carried out at room temperature. Liquid or solution transfers between reaction vessels were done via cannula. Solvents were dried by standard methods and distilled under argon or nitrogen immediately prior to use, or alternatively from a Solvent Purification System (Innovative Technologies). NMR spectra were recorded at 250, 300 or 400 MHz with Varian or Bruker spectrometers at variable temperature. Chemical shifts are reported in parts per million and referenced to $SiMe_4$ using the signal of the deuterated solvent (^1H) and (^{13}C) and 85% H_3PO_4 (^{31}P) as external reference, respectively. Elemental C, H and N analysis were performed in a Perkin-Elmer 2400 CHNS/O microanalyzer. Electrospray mass spectra (ESI-MS) were recorded on a Bruker MicroTof-Q at the Universidad de Zaragoza or on a LTQ-FT Ultra (Thermo Scientific) spectrometer at the Biomedical Research Institute (PCB-Universitat de Barcelona). MALDI-TOF mass spectra were obtained on a Bruker Miocroflex mass spectrometer using DCTB (*trans*-2-[3-(4-tert-butylphenyl)-2-methyl-2-propenylidene]malononitrile) or dithranol as matrix.

Standard literature procedures were used to prepare the starting materials $[Rh(\mu\text{-}Cl)(diolef)]_2$ (diolef = cod,[65] and nbd[66]), $[Ir(\mu\text{-}Cl)(cod)]_2$,[67] $[Rh(\mu\text{-}OMe)(cod)]_2$,[68] $[Rh(acac)(CO)(PPh_3)]$,[69] $[Pd(H_2O)_2(dppp)](OTf)_2$ (**c**)[70] and $[Pt(H_2O)_2(dppp)](OTf)_2$ (**d**).[70] The cationic complexes $[M(diolef)(NCCH_3)_2]BF_4$ (diolef = cod, M = Rh (**a**), Ir (**b**); diolef = nbd, M = Rh) were obtained following a slight modification of the literature procedure.[71] 4-pySH was purchased from Aldrich, recrystallized from methanol/diethyl ether and store under nitrogen.

Synthesis of $[Rh(\mu\text{-}4\text{-}Spy)(cod)]_2$ (1). *Method A*. A solution of *n*-BuLi (0.6 mL, 0.942 mmol, 1.57 M in hexanes) was slowly added to a yellow suspension of 4-pySH (0.096 g,

0.864 mmol) in THF (5 mL) at 273 K and the mixture stirred for 1 hour to give a white suspension of Li(4-Spy). Solid $[Rh(\mu\text{-}Cl)(cod)]_2$ (0.213 g, 0.432 mmol) was added to give an orange brown suspension that was stirred for 4 hours at room temperature. The solvent was removed under vacuum and the residue washed with cold methanol (2 x 3 mL) to give the compound as a brown solid that was filtered, washed with cold methanol and dried under vacuum. Yield: 0.216 g (78%). *Method B*. 4-pySH (0.230 g, 2.069 mmol) was added to a solution of $[Rh(\mu\text{-}OMe)(cod)]_2$ (0.500 mg, 1.032 mmol) in dichloromethane (15 mL) to give an orange solution that was stirred for 6 hours. The solution was concentrated under vacuum to *ca*. 2 mL and then diethyl ether (10 mL) was added to give a brown suspension. Further concentration and addition of diethyl ether gave the compound as a brown microcrystalline solid that was filtered, washed with diethyl ether (2 x 3 mL) and dried under vacuum. Yield: 0.556 g (84 %). Anal. Calcd for $C_{26}H_{32}N_2Rh_2S_2$ (%): C, 49.22; H, 3.81; N, 4.41; S, 10.10. Found: C, 49.02; H, 4.01; N, 4.35; S, 10.25. ^{1}H NMR (CD_2Cl_2, 298 K, 300.13 MHz) δ: 8.26 (dd, 4H, $J_{H\text{-}H}$ = 4.7 and 1.4 Hz, H_α), 7.28 (dd, 4H, $J_{H\text{-}H}$ = 4.7 and 1.4 Hz, H_β) (4-Spy), 4.45 (br s, 8H, =CH), 2.46 (br, 8H, $>CH_2$), 2.01 (br, 8H, $>CH_2$) (cod). ^{13}C NMR ($CDCl_3$, 298 K, 74.46 MHz) δ: 150.0 (*C*S), 148.9, 128.8 (4-Spy), 81.5 (d, $J_{C\text{-}Rh}$ = 11.7 Hz) (=CH), 31.6 ($>CH_2$) (cod). MS (ESI+, CH_2Cl_2, m/z): 853 $[Rh_3(Spy)_2(cod)_3]^+$ (3%), 643 $[Rh_2(SpyH)(Spy)(cod)_2]^+$ (25%), 433 $[Rh(SpyH)_2(cod)]^+$ (100%), 322 $[Rh(SpyH)(cod)]^+$ (60%).

Synthesis of $[Ir(\mu\text{-}4\text{-}Spy)(cod)]_2$ (2). $[Ir(\mu\text{-}Cl)(cod)]_2$ (0.352 g, 0.524 mmol) and Li(4-Spy), formed *in situ* by reaction of 4-pySH (0.117 g, 1.05 mmol) with *n*-BuLi (0.72 mL, 1.15 mmol, 1.6 M in hexanes), were reacted in THF (5 mL) for 10 hours. The yellow suspension was concentrated under vacuum and then methanol was added. The yellow solid was filtered, washed with methanol (3 x 4 ml) and dried under vacuum. Yield: 0.310 g (70%). Anal. Calcd for $C_{26}H_{32}N_2Ir_2S_2$ (%): C, 38.03; H, 3.93; N, 3.41; S, 7.81. Found: C, 38.15; H, 4.01; N, 3.36; S, 7.67. ^{1}H NMR (C_6D_6, 289K, 400.16 MHz) δ: 8.27 (br d, 4H, $J_{H\text{-}H}$ = 6.7 Hz, H_α), 6.99 (br d,

4H, J_{H-H} = 6.9 Hz, H_β) (4-Spy), 4.12 (br s, 8H, =CH), 2.01 (br, 8H, $>CH_2$), 1.52 (br, 8H, $>CH_2$) (cod). The ^1H NMR spectrum was obtained from a freshly prepared sample. On standing, the compound became insoluble in most of the usual organic solvents.

Synthesis of [Rh(μ-4-Spy)(nbd)]$_2$ (3). [Rh(μ-Cl)(nbd)]$_2$ (0.200 g, 0.434 mmol) and Li(4-Spy), formed *in situ* by reaction of 4-pySH (0.096 g, 0.868 mmol) with *n*-BuLi (0.6 ml, 0.942 mmol, 1.57 M in hexanes), were reacted in THF (5 mL) for 15 min at 273 K to give a brown suspension that was stirred for 4 hours. The solvent was removed under vacuum and the residue washed with cold methanol (2 x 3 mL) to give the compound as a brown solid that was filtered, washed with cold methanol and dried under vacuum. Yield: 0.190 g (72%). Anal. Calcd for $C_{24}H_{24}N_2Rh_2S_2$ (%): C, 47.22; H, 3.96; N, 4.59; S, 10.50. Found: C, 47.13; H, 4.01; N, 4.52; S, 10.35. ^1H NMR ($CDCl_3$, 298 K, 400.16 MHz) δ: 8.31(dd, 4H, J_{H-H} = 4.7 and 1.6 Hz, H_α), 6.97 (dd, 4H, J_{H-H} = 4.7 and 1.6 Hz, H_β) (4-Spy), 3.97 (s, 8H, =CH), 3.89 (s, 4H, CH), 1.36 (s, 4H, $>CH_2$) (nbd). MS (ESI+, CH_2Cl_2, m/z): 805 $[Rh_3(Spy)_2(nbd)_3]^+$ (15%), 611 $[Rh_2(SpyH)(Spy)(nbd)_2]^+$ (100%), 417 $[Rh(SpyH)_2(nbd)]^+$ (65%), 306 $[Rh(SpyH)(nbd)]^+$ (70%).

Synthesis of [Rh(μ-4-Spy)(CO)(PPh$_3$)]$_2$ (4). A solution of 4-pySH (0.045 g, 0.406 mmol) in CH_2Cl_2 (10 mL) was slowly added to a solution of [Rh(acac)(CO)(PPh_3)] (0.200 g, 0.406 mmol) in CH_2Cl_2 (10 mL). The solution was stirred for 1 hour to give a cloudy orange solution. The solvent was removed under vacuum and the residue extracted with a diethyl ether/CH_2Cl_2 (10:1) mixture (2 x 10 mL). The orange solution was filtered and concentrated under vacuum to *ca*. 1 mL. Slow addition of *n*-hexane (10 mL) and concentration gave a yellow solid. The precipitation was completed by addition of *n*-hexane and further concentration under vacuum. The yellow-orange solid was filtered, washed with *n*-hexane and dried under vacuum. Yield: 0.150 g (73%). Anal. Calcd for $C_{48}H_{38}N_2O_2P_2Rh_2S_2$ (%): C, 57.27; H, 3.80; N, 2.78; S, 6.37. Found: C, 57.26; H, 3.78; N, 2.66; S, 6.18. ^1H NMR ($CDCl_3$, 298 K,

300.13 MHz) δ: 8.39 (br s, 2H), 7.96 (br s, 2H), 7.85 (br s, 2H) (4-Spy), 7.56 (m, 12H), 7.38 (m, 6H), 7.28 (m, 12H) (Ph), 6.70 (br s, 2H, 4-Spy). $^{31}P\{^{1}H\}$ NMR ($CDCl_3$, 298 K, 121.48 MHz) δ: 38.26 (d, $J_{P\text{-}Rh}$ = 157.9 Hz). MS (ESI+, CH_2Cl_2, m/z): 1007 $[Rh_2(SpyH)(Spy)(CO)_2(PPh_3)_2]^+$ (60%), 615 $[Rh(SpyH)_2(CO)(PPh_3)]^+$ (100%). IR (CH_2Cl_2, cm^{-1}): ν(CO), 1983 (s).

Synthesis of $[\{Rh_2(\mu\text{-}4\text{-}Spy)_2(cod)_2\}_2\{Rh(cod)\}_2](BF_4)_2$ $(\mathbf{1a})_2$. Solid $[Rh(cod)(NCCH_3)_2]BF_4$ (0.041 g, 0.109 mmol) was added to a suspension of $[Rh(\mu\text{-}4\text{-}Spy)(cod)]_2$ (**1**, 0.070 g, 0.109 mmol) in THF (10 mL) to give an orange solution that was stirred for 2 hours. Concentration of the solution up to *ca*. 1 mL and slow addition of *n*-hexane (10 mL) gave the compound as a spongy orange solid that was filtered, washed with *n*-hexane (4 x 3 mL) and dried under vacuum. Yield: 0.064 g (62%). Anal. Calcd for $C_{68}H_{88}B_2F_8N_4Rh_6S_4$ (%): C, 43.43; H, 4.72; N, 2.98; S, 6.82. Found: C, 43.11; H, 4.90; N, 3.05; S, 6.90. ^{1}H NMR ($CDCl_3$, 298 K, 400.16 MHz) δ: 8.30 (d, 8H, $J_{H\text{-}H}$ = 6.6 Hz, H_α), 7.20 (d, 8H, $J_{H\text{-}H}$ = 6.6 Hz, H_β) (4-Spy), 4.79 (br s, 8H, =CH), 4.18 (br s, 8H, =CH), 3.97 (br s, 8H, =CH), 2.60 (br s, 16H, $>CH_2$), 2.36 (br s, 4H, $>CH_2$), 2.00 (br s, 4H, $>CH_2$), 1.98-1.86 (br s, 24H, $>CH_2$) (cod). ^{1}H NMR (CD_2Cl_2, 218 K, 300.13 MHz) δ: 8.12 (br s, 4H, H_α), 8.08 (br s, 4H, H_α), 7.52 (br s, 4H, H_β), 6.64 (br s, 4H, H_β) (4-Spy), 4.80 (br s, 4H, =CH), 4.68 (br s, 4H, =CH), 4.37 (br s, 4H, =CH), 3.93 (br s, 4H, =CH), 3.85 (br s, 8H, =CH), 2.47 (br s, 16H, $>CH_2$), 2.28 (br s, 8H, $>CH_2$), 2.10 (br s, 8H, $>CH_2$), 1.85 (br s, 16H, $>CH_2$) (cod). MS (ESI+, CH_2Cl_2, m/z): 1174 $[Rh_4(Spy)_3(cod)_4]^+$ (15%), 853 $[Rh_3(Spy)_2(cod)_3]^+$ (64%), 643 $[Rh_2(SpyH)(Spy)(cod)_2]^+$ (100%).

Synthesis of $[\{Ir_2(\mu\text{-}4\text{-}Spy)_2(cod)_2\}_2\{Ir(cod)\}_2](BF_4)_2$ $(\mathbf{2b})_2$. Solid $[Ir(cod)(NCCH_3)_2]BF_4$ (0.023 g, 0.049 mmol) was added to a yellow suspension of $[Ir(\mu\text{-}4\text{-}Spy)(cod)]_2$ (**2**, 0.040 g, 0.049 mmol) in THF (10 mL) and the mixture stirred overnight. The solvent was removed under vacuum and the residue washed with a CH_2Cl_2/diethyl ether (1:8) mixture (9 mL) to

give a deep red solid that was filtered, washed with diethyl ether (2 x 3 mL) and vacuum dried. Yield: 0.055 g (93%). Anal. Calcd for $C_{68}H_{88}B_2F_8Ir_6N_4S_4$ (%): C, 33.79; H, 3.67; N, 2.32; S, 5.30. Found: C, 33.50; H, 3.51; N, 2.28; S, 5.25. ^{1}H NMR (CD_2Cl_2, 298K, 400.16 MHz) δ: 8.28 (d, 8H, $J_{H\text{-}H}$ = 5.2 Hz, H_α), 7.33 (m, 8H, H_β) (4-Spy), 4.57 (br s, 8H, =CH), 3.95 (br s, 8H, =CH), 3.79 (br s, 8H, =CH), 2.43 (m, 16H, >CH_2), 2.06 (m, 4H, >CH_2), 1.81 (m, 4H, >CH_2), 1.62 (m, 24H, >CH_2) (cod). MS (MALDI-TOF, DIT matrix, CH_2Cl_2, m/z): 1121 $[Ir_3(Spy)_2(cod)_3]^+$.

Synthesis of [{Rh$_2$(μ-4-Spy)$_2$(cod)$_2$}$_2${Ir(cod)}$_2$](BF$_4$)$_2$ (1b)$_2$. Solid [Ir(cod)(NCCH$_3$)$_2$]BF_4 (0.029 g, 0.062 mmol) was added to an orange suspension of [Rh(μ-4-Spy)(cod)]$_2$ (**1**, 0.040 g, 0.062 mmol) in CH_2Cl_2 (10 mL) and the mixture stirred for 6 hours. Work up us described above for (**1a**)$_2$ gave the compound as a red solid. Yield: 0.045 g (70%). Anal. Calcd for $C_{68}H_{88}B_2F_8Ir_2N_4Rh_4S_4$ (%): C, 39.66; H, 4.30; N, 2.72; S, 6.23. Found: C, 39.48; H, 4.02; N, 2.65; S, 6.08. ^{1}H NMR (CD_2Cl_2, 298K, 400.16 MHz) δ: 8.27 (d, 4H, $J_{H\text{-}H}$ = 5.6 Hz, H_α), 8.20 (d, 4H, $J_{H\text{-}H}$ = 5.6 Hz, H_α), 7.20 (br s, 8H, H_β) (4-Spy), 4.77 (br s, 4H, =CH), 4.54 (br s, 4H, =CH) (Rh-cod), 4.27 (br s, 8H, =CH), 4.00 (br s, 8H, =CH) (Rh-cod and Ir-cod), 2.59 (m, 12H, >CH_2), 2.48 (m, 16H, >CH_2), 1.97 (m, 12H, >CH_2), 1.55 (m, 8H, >CH_2) (cod). MS (MALDI-TOF, DIT matrix, CH_2Cl_2, m/z): 943 $[Rh_2Ir(Spy)_2(cod)_3]^+$.

Synthesis of [{Rh$_2$(μ-4-Spy)$_2$(cod)$_2$}$_2${Pd(dppp)}$_2$](OTf)$_4$ (1c)$_2$. Solid [Pd(H$_2$O)$_2$(dppp)](OTf)$_2$ (0.027 g, 0.030 mmol) was added to a CH_2Cl_2 solution (5 mL) of [Rh(μ-4-Spy)(cod)]$_2$ (**1**, 0.020 g, 0.030 mmol). After 2h of stirring, the reaction mixture was filtered, concentrated to 5 mL under vacuum and precipitated with *n*-hexane. A yellow solid was obtained. Yield: 0.035 g (78 %). Anal. Calcd for $C_{110}H_{116}N_4Pd_2P_4Rh_4O_{12}F_{12}S_8$: C, 45.26; H, 4.01; N, 1.92; S, 8.79. Found: C, 45.43; H, 3.98; N, 1.95; S, 8.70. ^{1}H NMR ($CDCl_3$, 298 K, 250.13 MHz) δ: 8.33 (br s, 8H, H_α) (4-Spy), 7.57 (m, 16H), 7.32 (m, 24H) (Ph), 6.74 (d, 8H, $J_{H\text{-}H}$ = 5.0 Hz, H_β) (4-Spy), 4.67 (br s, 8H, =CH), 3.98 (br s, 8H, =CH) (cod), 3.15 (m, 8H, P-

CH_2-C) (dppp), 2.56 (br s, 8H, >CH_2), 2.36 (br s, 8H, >CH_2) (cod), 2.10 (m, 20H) (>CH_2 cod + C-CH_2-C dppp). $^{31}P\{^1H\}$ NMR ($CDCl_3$, 298K, 101.25 MHz) δ: 6.5 s. HRMS (ESI+, acetone, m/z): 1311.1 $[\{Rh_2(Spy)_2(cod)_2\}_2\{Pd(dppp)\}_2(OTf)_2]^{2+}$ (90%), 823.7 $[\{Rh_2(Spy)_2(cod)_2\}_2\{Pd(dppp)\}_2(OTf)]^{3+}$ (8%).

Synthesis of $[\{Rh_2(\mu\text{-}4\text{-}Spy)_2(cod)_2\}_2\{Pt(dppp)\}_2](OTf)_4$ $(\mathbf{1d})_2$. Solid $[Pt(H_2O)_2(dppp)](OTf)_2$ (0.029 g, 0.030 mmol) was added to a CH_2Cl_2 solution (5 mL) of $[Rh(\mu\text{-}4\text{-}Spy)(cod)]_2$ (**1**, 0.020 g, 0.030 mmol) and the mixture stirred for 2 hours. Work up us described above for $(\mathbf{1c})_2$ gave the compound as an orange solid. Yield: 0.039 g (80 %). Anal. Calcd for $C_{110}H_{116}N_4Pt_2P_4Rh_4O_{12}F_{12}S_8$: C, 42.67; H, 3.78; N, 1.81; S, 8.28. Found: C, 42.81; H, 3.81; N, 1.76; S, 8.19. ^1H NMR (CD_2Cl_2, 298 K, 500.13 MHz) δ: 8.28 (d, 8H, $J_{H\text{-}H}$ = 5.0 Hz, H_α) (4-Spy), 7.59 (m, 16H), 7.35 (m, 24H) (Ph), 6.78 (d, 8H, $J_{H\text{-}H}$ = 5.0 Hz, H_β) (4-Spy), 4.65 (br s, 8H, =CH), 4.05 (br s, 8H, =CH) (cod), 3.21 (m, 8H, P-CH_2-C) (dppp), 2.54 (m, 8H, >CH_2), 2.40 (br s, 8H, >CH_2) (cod), 2.14 (m, 12H) (>CH_2 cod + C-CH_2-C dppp), 2.03 (m, 8H, >CH_2) (cod). $^{31}P\{^1H\}$ NMR ($CDCl_3$, 298K, 101.25 MHz) δ: -14.5 (s, $J_{P\text{-}Pt}$ = 2989 Hz). HRMS (ESI+, acetone, m/z): 1399.1 $[\{Rh_2(Spy)_2(cod)_2\}_2\{Pt(dppp)\}_2(OTf)_2]^{2+}$ (100%); 882.7 $[\{Rh_2(Spy)_2(cod)_2\}_2\{Pd(dppp)\}_2(OTf)]^{3+}$ (30%).

Synthesis of $[\{Ir_2(\mu\text{-}4\text{-}Spy)_2(cod)]_2\}_2\{Pd(dppp)\}_2](OTf)_4$ $(\mathbf{2c})_2$. Solid $[Pd(H_2O)_2(dppp)](OTf)_2$ (0.026 g, 0.030 mmol) was added to a CH_2Cl_2 suspension (5 mL) of $[Ir(\mu\text{-}4\text{-}Spy)(cod)]_2$ (**2**, 0.025 g, 0.030 mmol) and the mixture stirred for 2 hours. Work up us described above for $(\mathbf{1c})_2$ gave the compound as an orange solid. Yield: 0.037 g (75 %). Anal. Calcd for $C_{110}H_{116}N_4Pd_2P_4Ir_4O_{12}F_{12}S_8$: C, 40.33; H, 3.57; N, 1.71; S, 7.83. Found: C, 40.57; H, 3.54; N, 1.70; S, 7.90. ^1H NMR ($CDCl_3$, 298 K, 250.13 MHz) δ: 8.46 (br s, 8H, H_α) (4-Spy), 7.67 (m, 16H), 7.32 (m, 24H) (Ph), 6.78 (br s, 8H, H_β) (4-Spy), 4.41 (br s, 8H, =CH), 3.65 (br s, 8H, =CH) (cod), 3.16 (br s, 8H, P-CH_2-C) (dppp), 2.80-1.90 (m, 36H) (>CH_2 cod + C-CH_2-C (dppp)). $^{31}P\{^1H\}$ NMR ($CDCl_3$, 298K, 101.25 MHz) δ: 6.5 s. HRMS (ESI+, acetone, m/z):

3127.2 $[\{Ir_2(Spy)_2(cod)_2\}_2\{Pd(dppp)\}_2(OTf)_3]^+$ (1%); 1489.2 $[\{Ir_2(Spy)_2(cod)_2\}_2\{Pd(dppp)\}_2(OTf)_2]^{2+}$ (100%); 943.1 $[\{Ir_2(Spy)_2(cod)_2\}_2\{Pd(dppp)\}_2(OTf)]^{3+}$ (5%).

Synthesis of $[\{Ir_2(\mu\text{-}4\text{-}Spy)_2(cod)]_2\}_2\{Pt(dppp)\}_2](OTf)_4$ $(2d)_2$. Solid $[Pt(H_2O)_2(dppp)](OTf)_2$ (0.023 g, 0.020 mmol) was added to a CH_2Cl_2 suspension (5 mL) of $[Ir(\mu\text{-}4\text{-}Spy)(cod)]_2$ (**2**, 0.020 g, 0.020 mmol) and the mixture stirred for 2 hours. Work up us described above for $(\mathbf{1c})_2$ gave the compound as a red solid. Yield: 0.029 mg (70 %). Anal. Calcd for $C_{110}H_{116}N_4Pt_2P_4Ir_4O_{12}F_{12}S_8$: C, 38.26; H, 3.38; N, 1.62; S, 7.43. Found: C, 37.95; H, 3.34; N, 1.68; S, 7.50. ^{1}H NMR ($CDCl_3$, 298 K, 250.13 MHz) δ: 8.50 (d, 8H, $J_{H\text{-}H}$ = 2.5 Hz, H_α) (4-Spy), 7.68-7.34 (m, 40H) (Ph), 6.83 (d, 8H, $J_{H\text{-}H}$ = 5.0 Hz, H_β) (4-Spy), 4.41 (br, 8H, =CH), 3.68 (m, 8H, =CH) (cod), 3.27 (m, 8H, P-CH_2-C) (dppp), 2.43 (br, 16H >CH_2) (cod), 2.01 (br m, 20H) (>CH_2 cod + C-CH_2-C dppp). $^{31}P\{^1H\}$ NMR ($CDCl_3$, 298K, 101.25 MHz) δ: -14.9 (s, $J_{P\text{-}Pt}$ = 3054 Hz). HRMS (ESI+, acetone, m/z): 3303.4 $[\{Ir_2(Spy)_2(cod)_2\}_2\{Pd(dppp)\}_2(OTf)_3]^+$ (1%); 1577.7 $[\{Ir_2(Spy)_2(cod)_2\}_2\{Pd(dppp)\}_2(OTf)_2]^{2+}$ (50%); 1002.1 $[\{Ir_2(Spy)_2(cod)_2\}_2\{Pd(dppp)\}_2(OTf)]^{3+}$ (15%).

Crystal Structure Determination of $[\{Rh_2(\mu\text{-}4\text{-}Spy)_2(cod)_2\}_2\{Rh(cod)\}_2](BF_4)_2$ $(\mathbf{1a})_2$ and $[\{Rh_2(\mu\text{-}4\text{-}Spy)_2(cod)_2\}_2\{Pt(dppp)\}_2](OTf)_4$ $(\mathbf{1d})_2$. Data for $(\mathbf{1a})_2$ were collected at 150(1)K from a BrukerAXS SMART APEXII CCD diffractometer at 9.8 station of the SRS Daresbury laboratory. Radiation was monochromated with a silicon 111 crystal (λ = 0.69340 Å). X-ray diffraction data for $(\mathbf{1d})_2$ were collected at 100(2)K with graphite-monochromated Mo-Kα radiation (λ = 0.71073 Å) on a Bruker SMART APEX CCD diffractometer. In both cases, ω narrow rotation (0.3°) scans were used, and the measured intensities were integrated and corrected for the absorption effect with SAINT+[72] and SADABS[73] programs. Structures were solved by direct methods with SHELXS-97.[74,75] Refinement was carried out by full-matrix least-squares on F^2 for all data with SHELXL-97.[76] All hydrogen atoms were calculated and

refined using a riding model. PARST program[77,78] was used in the geometrical analysis of the complexes.

Although several crystals were tested, data for $(\mathbf{1a})_2$ showed in all cases broad reflections with general low intensity most probably due to quick loss of solvent for these samples. The eventual data collected prevented a proper conventional least-square refinement, but allow the appropriate identification of the metallocyclic skeleton of the molecule. A similar situation has been described for other related macromolecular complexes where big cavities contain very labile and/or disordered solvent molecules.[79-83] The limited quality of crystal data of $(\mathbf{1a})_2$ does not allow a conventional refinement of all non-hydrogen atoms including anisotropic thermal parameters. The atoms of the counterions (found to be disordered) have been refined with isotropic thermal parameters and a common thermal parameter has been used for the fluorine atoms; geometrical restraints for both B-F bond lengths and F-B-F angles were also applied. Moreover, some additional restraints in ADPs have been defined for some bonds of cod ligands to ensure fulfillment of the Hirshfeld test. Finally, one of the pyridine rings has been found to be disordered; atoms of this group have been included in the model in two sets of positions and isotropically refined with complementary occupancy factors (0.59 / 0.41(2)) including geometrical restraints.

At the final steps of both structural refinements, clear evidence of the existence of large solvent-accessible voids and the presence of highly disordered solvent was observed. All attempts to model these molecules were unsuccessful. An analysis of the solvent region has therefore been performed using SQUEEZE program.[84] The contribution of the estimated solvent content to the total structure factors has been calculated and incorporated in further least-squares refinements. A summary of the crystal data and structure refinement parameters is reported in Table 1.

Table 1. Crystal Data and Structure Refinement.

	$(1a)_2$	**$(1d)_2$**
Molecular formula	$C_{69}H_{90}N_4Rh_6S_4$, 2(BF_4), CH_2Cl_2, 1.25(C_6H_{14})	$C_{106}H_{116}N_4P_4Pt_2Rh_4S_4$, 4($CF_3O_3S$), 4($CH_2Cl_2$), 7($C_4H_{10}O$)
Formula weight	2073.39	3954.79
Temp (K)	150	100
λ (Å)	0.6934	0.73071
Crystal system	Monoclinic	Monoclinic
Space group	*C*2/c	$P2_1/n$
a (Å)	39.803(4)	14.4510(9)
b (Å)	16.5686(16)	18.3763(11)
c (Å)	28.098(3)	27.5849(17)
β (º)	115.516(2)	90.8530(10)
V ($Å^3$)	16723(3)	7324.5(8)
Z	8	2
μ (mm^{-1})	1.174	2.729
D_{calc} (g/cm^3)	1.647	1.793
F(000)	8356	3988
Crystal dimensions (mm)	0.01 x 0.03 x 0.08	0.05 x 0.07 x 0.08
T_{min}/ T_{max}	0.627 / 1	0.598 / 0.746
Collected/unique reflections	50004 / 11966	47211 / 16801
R_{int}	0.1101	0.0458
Data/restraints/parameters	11966 / 188 / 783	16801 / 2 / 755
R_1 [I > 2σ(I)][a]	0.1028	0.0480
wR_2 (all data)[b]	0.3229	0.1336

[a] $R_1 = \frac{|Fo| - |F_C|}{|Fo|}$; [b] $wR_2 = \sqrt{\frac{w(F_O^2 - F_C^2)^2}{w(F_O^2)^2}}$

Results and discussion

Synthesis of dinuclear rhodium and iridium [M(μ-4-Spy)(diolef)]$_2$ ditopic metalloligands. The synthesis of bimetallic metalloligands containing pyridine-4-thiolato ligands was readily accomplished following two procedures described in the literature by our group. The first one[43] makes use of the lithium salt Li(4-Spy), which was prepared *in situ* by reaction of 4-pySH with *n*-BuLi in THF (method A). As shown in Scheme 1, reaction of Li(4-Spy) with compounds [M(μ-Cl)(cod)]$_2$ in a 2:1 molar ratio led to the formation of the thiolate-bridged complexes [M(μ-4-Spy)(cod)]$_2$ (M = Rh (**1**), Ir (**2**)), which were isolated as air sensitive orange-brown (**1**) or yellow-brown (**2**) solids in good yield. While compound **1** is soluble in most of the common organic solvents, the iridium derivative **2** shows a limited solubility in all of them. Compound **1**, was obtained in similar yield by an alternative method[45] that involves the direct protonation of the methoxide bridging ligands in complex [Rh(μ-OMe)(cod)]$_2$ by 4-pySH in dichloromethane (method B).

The binuclear compounds **1** and **2** were characterized by elemental analysis, mass spectrometry (ESI+), and NMR spectroscopy. The MS (ESI+) spectrum of **1** in CH_2Cl_2 displayed the peak corresponding to the dinuclear protonated $[(\mathbf{1})_2 + H]^+$ species at *m*/*z* 643 that supports the formation of the desired compound. In spite of numerous attempts, (ESI(+), FAB(+) and MALDI-TOF in different solvents), mass spectrometry did not provide confirmation of the nuclearity of compound **2**. However, satisfactory mass spectra were obtained when the dinuclear iridium compound is a constituent of the supramolecular assemblies that will be described later on.

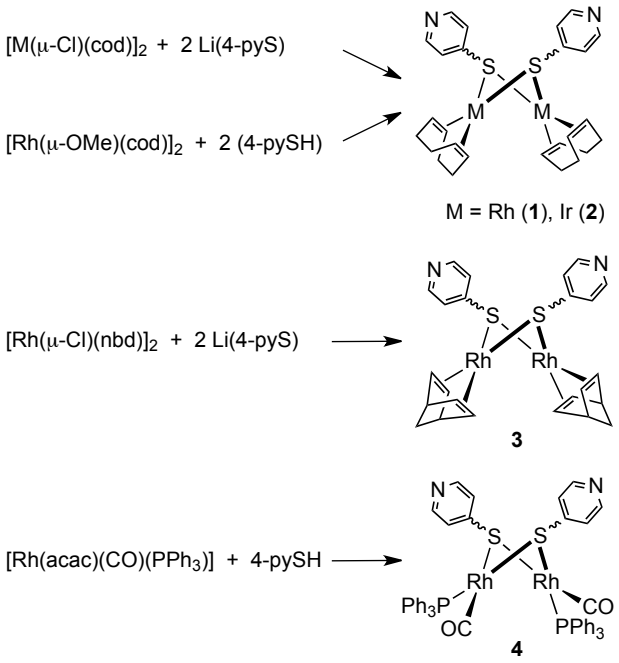

Scheme 1. Preparation of dinuclear thiolate-bridged rhodium and iridium metalloligands.

The room temperature ^{1}H NMR spectra of both **1** and freshly prepared **2** (in CD_2Cl_2 and C_6D_6 respectively), showed the expected signals for the α and β protons of the pyridine rings as well as those attributable to =CH and >CH_2 protons of the 1,5-cyclooctadiene ligand that were observed as a set of broad resonances. The =CH protons were observed as a single resonance at δ 4.45 and 4.12 ppm for **1** and **2,** respectively. The two resonances at δ 2.46 and 2.01 for **1** and 2.01 and 1.52 for **2**, were assigned to the non-equivalent protons within each of the >CH_2 groups (*exo* and *endo* protons). The straightforward pattern is indicative of the high symmetry of the obtained species. This simplicity could be also found in the ^{13}C{^{1}H} NMR spectrum of **1 (**the spectrum of **2** could not be registered due to its low solubility) where, apart from the three resonances assigned to the pyridine carbons, only one doublet for the olefinic =CH groups (81.5 ppm, $J_{C\text{-}Rh}$ = 11.7 Hz) and a single resonance for the >CH_2 carbons (31.6 ppm) were observed for the 1,5-cyclooctadiene ligands. The features of the ^{1}H NMR spectrum suggest a fluxional behavior derived from an open-book structure resulting from the μ-(1:2κ^{2}S) coordination mode of both pyridine-4-thiolato ligands with a *syn* disposition. In fact,

the inversion of the non-planar Rh_2S_2 ring accounts for the equivalence of all the olefinic =CH protons and carbons at room temperature.[43,45,85-87] Interestingly, a number of thiolate-bridged dinuclear rhodium and iridium complexes containing cyclooctadiene ligands display a *syn-endo* conformation in the solid state and exhibit a dynamic behavior similar to that found in complex **1**.[45,86-89] Unfortunately, the ^{1}H NMR spectrum was not resolved even at 193 K, which points to a low-energy ring inversion process.

A dirhodium compound analogous to **1** but containing 2,5-norbornadiene ligands was also synthesized. $[Rh(\mu\text{-Spy})(nbd)]_2$ (**3**) was obtained from $[Rh(\mu\text{-Cl})(nbd)]_2$ and Li(4-Spy) as a brown solid in good yields (Scheme 1). Its characterization by elemental analysis, NMR spectroscopy and mass spectrometry confirmed its analogy with compound **1**. In fact, its ^{1}H NMR spectrum also evidenced a fluxional behavior that renders equivalent the =CH and CH protons of both nbd ligands.

Treatment of the mononuclear complex $[Rh(acac)(CO)(PPh_3)]$ with one equivalent of 4-pySH in dichloromethane gave a deeply orange solution from which the dinuclear compound $[Rh(\mu\text{-4-Spy})(CO)(PPh_3)]_2$ (**4**) was isolated as a yellow-orange solid in good yield. Complex **4** was characterized by elemental analysis, mass spectrometry and IR and NMR spectroscopies. The dinuclear formulation of compound **4** relies on the ESI+ mass spectrum, which showed the protonated molecular cation $[Rh_2(SpyH)(Spy)(CO)_2(PPh_3)_2]^+$ at *m/z* 1007.

The ^{1}H NMR spectrum of **4** in $CDCl_3$ also featured broad resonances although in this case the pyridine-4-thiolato ligands were not equivalent and showed four resonances at δ 8.39, 7.96, 7.85 and 6.70 ppm. The $^{31}P\{^1H\}$ NMR spectrum was in accordance with the equivalence of both triphenylphosphine ligands because only a doublet due to the coupling with the rhodium nucleus was observed ($^1J_{P\text{-}Rh}$ = 158 Hz). The inequivalence of the bridging ligands suggests a dinuclear structure with a *cis* disposition of the bulky triphenylphosphine ligands. Most probably, the thiolato ligands display an *anti* conformation with the *endo* substituent at

the side of the molecule with the small carbonyl ligands as is usually found in related complexes.[45]

General strategy for self-assembly reactions. Once prepared and fully characterized, the bimetallic metalloligands described above were used to design self-assembled metallomacrocycles. The thiolate-bridged dinuclear compounds feature two peripheral pyridine nitrogen donor atoms available for coordination to suitable metal fragments. However, giving the lack of conformational rigidity of this family of compounds, different possibilities of self-assembly could be envisaged depending on the relative disposition of the pyridine rings (Figure 1). This feature provides highly flexible linkages for the design of supramolecular assemblies.

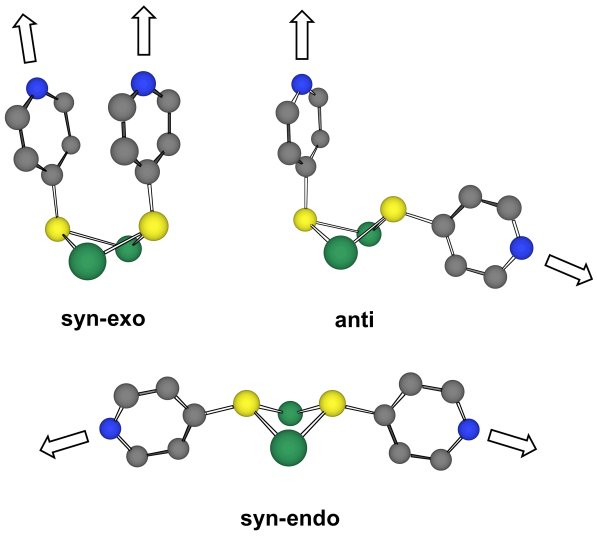

Figure 1. Different isomers arising from the relative disposition of the pyridine rings in the thiolate-bridged dinuclear metalloligands.

While the *syn-exo* isomer could yield discrete metallomacrocycles as a result of its combination with metal building blocks having two available coordination sites at 180°, acceptor units having two coordination positions at 90° should be necessary in order to get a discrete assembly in the case of the *syn-endo* isomer, which displays an almost linear orientation of the pyridine fragments. The *anti* isomer, however, has the possibility of

forming discrete species either by combination with 90° or 180° acidic metal fragments. Nevertheless, it has to be considered that the disposition of the donor moieties in these metalloligands does not allow ruling out the formation of self-assembled polymeric species such infinite chains or networks.

Although the choice of a metal-containing acceptor with an adequate angle between the vacant positions may be decisive for the control of the reactivity at the metal site, the nature of the final products will depend on their thermodynamic stability since it is know that self-assembly is a thermodynamically controlled process. As we have pointed above, we chose two different types of acceptor building blocks *i. e.* $[M(diolef)(CH_3CN)_2]^+$ (diolef = cod, nbd; M = Rh, Ir) and $[M(H_2O)_2(dppp)]^{2+}$ (M = Pd, Pt), where two adjacent coordination positions are blocked by bidentate ligands in order to assure an angle of 90° between the acidic sites.

Self–assembly reactions involving $[M(\mu\text{-Spy})(cod)]_2$ (M = Rh (1), Ir (2)) metalloligands and $[M(diolef)(CH_3CN)_2]^+$ (diolef = cod, nbd; M = Rh (a), Ir (b)) acceptor units. The bimetallic pyridine-4-thiolate-bridged compounds $[M(\mu\text{-Spy})(cod)]_2$ (M = Rh (**1**), Ir (**2**)) were found to undergo self-assembly with both solvent-stabilized species $[M(cod)(NCCH_3)_2]^+$ (M = Rh (**a**) and M = Ir (**b**)) in dichloromethane at room temperature to give exclusively the rectangular hexanuclear metallomacrocycles $(\mathbf{1a})_2$, $(\mathbf{1b})_2$ and $(\mathbf{2b})_2$ as shown in Scheme 2.

After the reaction completion (2h for $(\mathbf{1a})_2$ and $(\mathbf{1b})_2$, and 12h for $(\mathbf{2b})_2$), the species were obtained as solids in moderate to good yields (60-90%) and characterized by elemental analysis, mass spectrometry (ESI+ or MALDI) and NMR spectroscopy. In addition, single crystals of compound $(\mathbf{1a})_2$ were grown by slow diffusion of hexane into a dichloromethane solution of the complex at 258 K and were further characterized by an X-ray diffraction analysis.

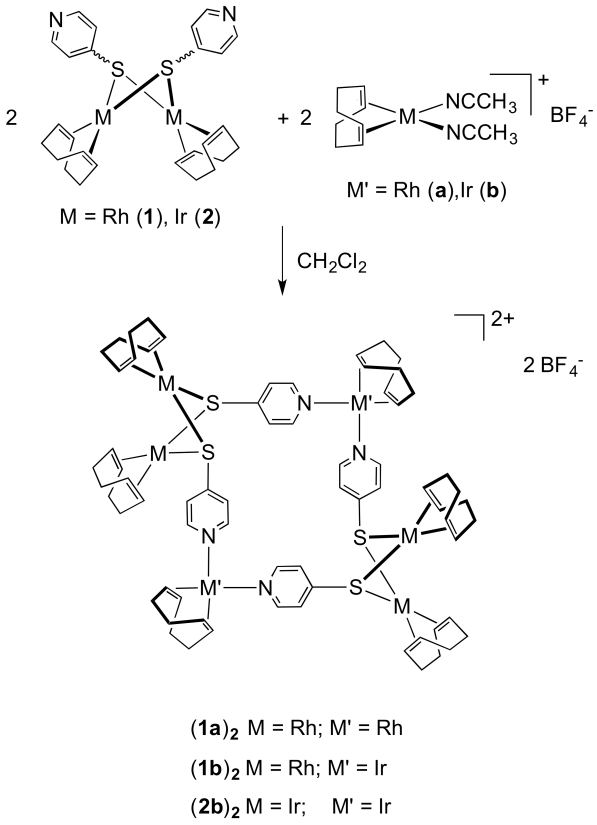

Scheme 2. Self-assembly of hexanuclear rhodium and iridium metallomacrocycles

A molecular representation of the cation of $(\mathbf{1a})_2$ is depicted in Figure 2, and selected structural parameters are summarized in Table 2. Rhodium atoms of both bimetallic [Rh(μ-4-SPy)(cod)]$_2$ fragments display a slightly distorted square-planar geometry resulting from the coordination of sulfur atoms of two pyridine-4-thiolato ligands and a cod molecule chelated through the two olefinic bonds. Similar acute S-Rh-S angles (in the range 79.49(17)-80.68(15)º) and *trans*-angles S-Rh-G (G being the centroid of the olefinic C=C bonds) close to 180º (167.4(6)-177.0(6)º) are observed. Rhodium atoms are slightly displaced out of their coordination mean plane (Rh(1): 0.111(1), Rh(2): 0.074(1), Rh(3): 0.008(2) and Rh(4): 0.114(2) Å), evidencing the distortion from an ideal square-planar conformation, as previously observed in related thiolate bridged Rh(I) complexes.[47] Central Rh_2S_2 cores are folded, as indicated by the hinge angle between the two rhodium coordination planes (78.1(2) and 75.4(3)º for Rh(1)-S(2)-Rh(2)-S(4) and Rh(3)-S(1)-Rh(4)-S(3) bimetallic fragments,

respectively). Long intermetallic distances of 2.924(3) and 2.965(3) Å are found, excluding metal-metal interactions. Both the dihedral angles and interatomic distances nicely agree with values reported for related compounds as [Rh(μ-2,3,5,6-tetrafluoro-4-(trifluoromethyl)-benzenethiolato)(cod)]$_2$ (73.85º and 2.9595(3) Å),[90] [{Rh(cod)}$_2$(μ-S,S-EtSNS)]OTf (EtSNS = EtNC(S)Ph$_2$P=NPPh$_2$C(S)NEt (77.56º and 2.942 Å)[91] or [Rh(μ_2-methylthiolato)(cod)]$_2$ (75.86º and 2.947 Å).[89]

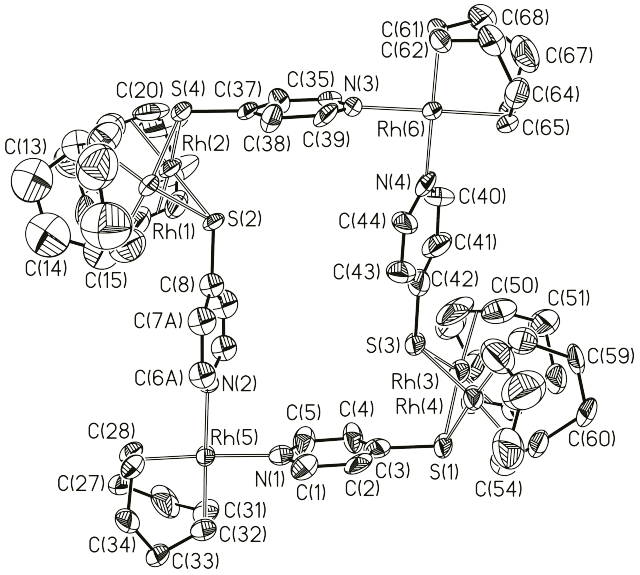

Figure 2. Molecular structure of the cation of (**1a**)$_2$, drawn at 40% probability level. For clarity, hydrogen atoms and the minor component of the disordered pyridine ring have been omitted.

Table 2. Selected bond lengths (Å) and angles (º) for $(\mathbf{1a})_2$.

Rh(1)-S(2)	2.380(5)	S(2)-Rh(1)-S(4)	80.68(15)	S(1)-Rh(3)-S(3)	79.49(17)
Rh(1)-S(4)	2.366(5)	S(2)-Rh(1)-G(1)	167.4(6)	S(1)-Rh(3)-G(7)	176.6(7)
Rh(2)-S(2)	2.387(5)	S(2)-Rh(1)-G(2)	101.7(7)	S(1)-Rh(3)-G(8)	92.7(7)
Rh(2)-S(4)	2.366(4)	S(4)-Rh(1)-G(1)	88.7(5)	S(3)-Rh(3)-G(7)	102.0(9)
Rh(3)-S(1)	2.377(6)	S(4)-Rh(1)-G(2)	174.8(6)	S(3)-Rh(3)-G(8)	172.0(8)
Rh(3)-S(3)	2.384(5)	G(1)-Rh(1)-G(2)	88.3(8)	G(7)-Rh(3)-G(8)	85.9(11)
Rh(4)-S(1)	2.383(5)	S(2)-Rh(2)-S(4)	80.55(15)	S(1)-Rh(4)-S(3)	79.71(15)
Rh(4)-S(3)	2.366(5)	S(2)-Rh(2)-G(3)	101.1(5)	S(1)-Rh(4)-G(9)	92.9(8)
Rh(5)-N(1)	2.105(13)	S(2)-Rh(2)-G(4)	170.1(5)	S(1)-Rh(4)-G(10)	167.6(7)
Rh(5)-N(2)	2.151(10)	S(4)-Rh(2)-G(3)	177.0(6)	S(3)-Rh(4)-G(9)	172.6(6)
Rh(6)-N(3)	2.094(12)	S(4)-Rh(2)-G(4)	91.1(6)	S(3)-Rh(4)-G(10)	98.9(6)
Rh(6)-N(4)	2.047(13)	G(3)-Rh(2)-G(4)	86.9(8)	G(9)-Rh(4)-G(10)	88.5(9)
Mean Rh-G[a]	2.017(6)	N(1)-Rh(5)-N(2)	88.4(4)	N(3)-Rh(6)-N(4)	88.3(4)
		N(1)-Rh(5)-G(5)	177.2(5)	N(3)-Rh(6)-G(11)	178.0(5)
		N(1)-Rh(5)-G(6)	90.6(6)	N(3)-Rh(6)-G(12)	91.9(5)
		N(2)-Rh(5)-G(5)	93.5(5)	N(4)-Rh(6)-G(11)	91.8(6)
		N(2)-Rh(5)-G(6)	176.8(6)	N(4)-Rh(6)-G(12)	178.1(6)
		G(5)-Rh(5)-G(6)	87.6(7)	G(11)-Rh(6)-G(12)	88.1(6)

[a] G(n) represent the centroids of the olefinic bonds of cod ligands.

The bimetallic metalloligands with a bent-*anti* arrangement, coordinate to Rh(cod) fragments giving rise to hexanuclear metallomacrocycles exhibiting an unusual alternating disposition of bi- and mono- metallic corners. The *anti* disposition of the thiolato ligands in the dinuclear rhodium corners contrasts with the *syn* disposition observed in the parent dinuclear thiolate-bridged building block (see above). As the *syn-anti* interconversion cannot be explained by inversion of the non-planar Rh_2S_2 ring, the formation of the metallomacrocycles should involve a sulfur inversion. This can occur either by breaking of a

Rh-S bond (dissociative mechanism) or through a planar transition state in which the S atom is sp^2-hybridized (non-dissociative mechanism).[52]

The Rh(5) and Rh(6) metal centers at the mononuclear corners also display a square-planar coordination, less distorted than those of the metal atoms of the bimetallic fragments (out-of-plane distances: 0.008(1) and 0.001(2) Å, for Rh(5) and Rh(6), respectively). N(1)-Rh(5)-N(2) and N(3)-Rh(6)-N(4) angles, very close to 90º, generate a rectangular molecule core, whose dimensions can be roughly estimated from Rh(5)···S(1)···Rh(6)···S(4) distances as 6.641(3) x 9.613(4) Å (Figure 3). The mean plane of the metallomacrocycle, defined by Rh(5), Rh(6), sulfur and nitrogen atoms is almost parallel to the (*b*, *c*) crystallographic plane.

The conformational geometry, with pyridine-4-thiolato ligands as intermetallic linkers, induces rhodium atoms of bimetallic fragments to be placed above and below this mean plane, respectively, with the bulkiest cod ligands being located in the outer part of the metallomacrocycle. Apparently, no steric impediment seems to hinder the accessibility to the metallomacrocyclic cavity. Along the a axis, the structure shows the presence of pair of molecules, with the metallomacrocycles in a parallel disposition but twisted 90 degrees one respect to the other (Figure 4). Minimal distances between Rh atoms within a pair and between pairs are 7.668(2) Å and 7.212(2) Å, respectively.

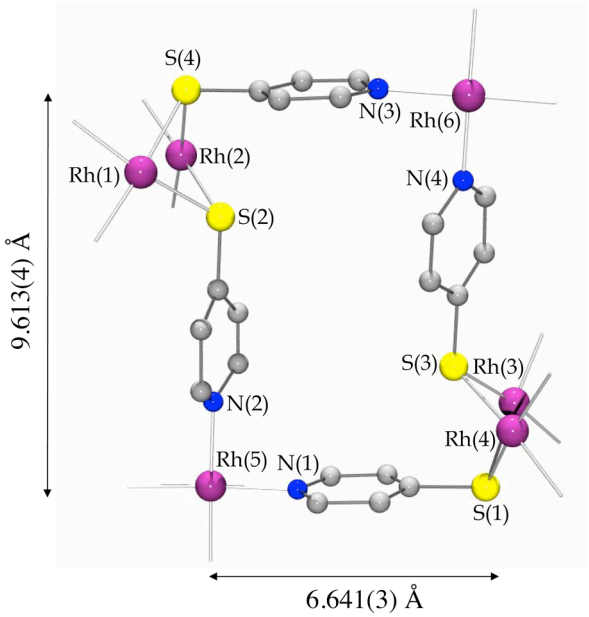

Figure 3. Schematic view of the rectangular molecular core of $(\mathbf{1a})_2$.

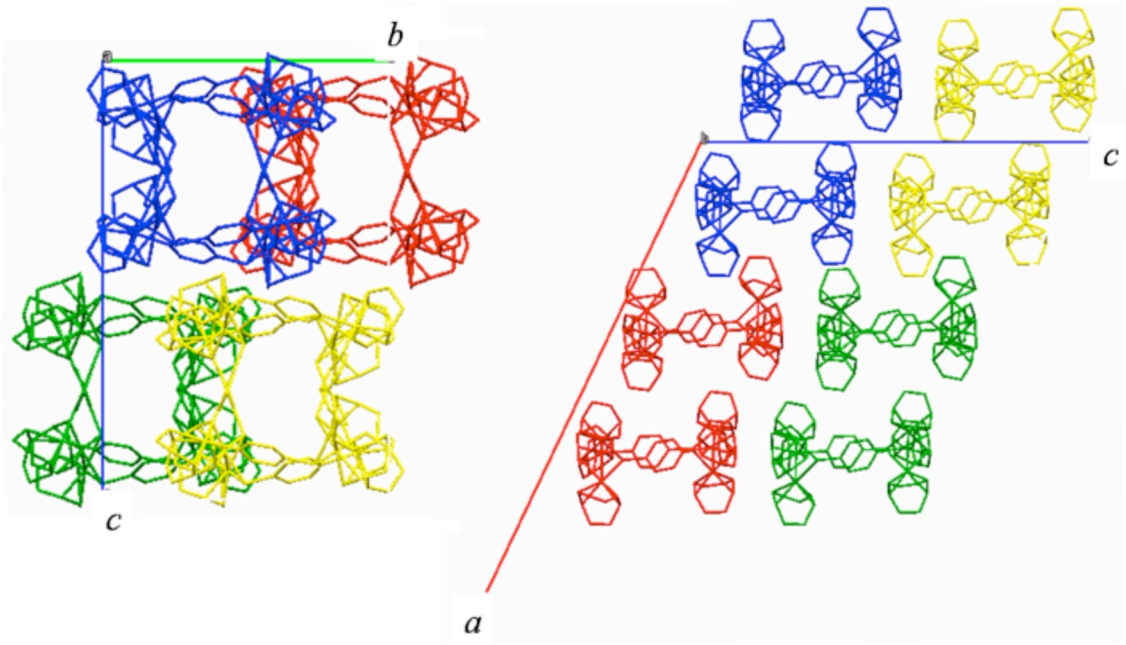

Figure 4. Molecular packing of $(\mathbf{1a})_2$ along crystallographic *a* and *b* axis. To properly show the cavity, counterions and solvent have been omitted. Different colors are used to identify pair of molecules with overlapping metallomacrocycles.

Interestingly, the coordination chemistry of complexes $[M(\mu\text{-4-Spy})(cod)]_2$, that results in the formation of the macrocyclic species, contrasts with that of related dinuclear

thiophenolato-bridged complexes $[M(\mu\text{-SPh})(cod)]_2$ (M = Rh, Ir). The later reacted with solvent stabilized cationic $[M(cod)L_2]^+$ fragments to give cationic trinuclear aggregates $[M_3(\mu\text{-SPh})_2(diolef)_3]^+$ which are formed by a triangular arrangement of metal atoms capped on each side by two triply bridging phenylthio ligands.[43] These species showed an outstanding stability and, in fact, related trinuclear ions, that corresponds to the half of the self-assembled species, were observed in the mass spectrum of the three macrocyclic compounds $(\mathbf{1a})_2$, $(\mathbf{1b})_2$ and $(\mathbf{2b})_2$, *i.e.* $[Rh_3(Spy)_2(cod)_3]^+$ (*m/z* = 853), $[Rh_2Ir(Spy)_2(cod)_3]^+$ (*m/z* = 943) and $[Ir_3(Spy)_2(cod)_3]^+$ (*m/z* = 1221), respectively.

On the other hand, the ^{1}H NMR spectra at room temperature of the obtained compounds (Supporting Information, Figures **S1-S6**) were in agreement with the existence of a single species that undergoes a dynamic process in solution. Indeed, the metallomacrocycles $[\{M_2(\mu\text{-4-Spy})_2(cod)_2\}_2\{M'(cod)\}_2]^{2+}$ (M = M'= Rh $(\mathbf{1a})_2$; M = Rh, M' = Ir $(\mathbf{1b})_2$; M = M' = Ir $(\mathbf{2b})_2$) are fluxional as was evidenced by a NMR study at variable temperature. The ^{1}H NMR spectrum of $[\{Rh_2(\mu\text{-4-Spy})_2(cod)_2\}_2\{Rh(cod)\}_2]^{2+}$ $(\mathbf{1a})_2$ at 218 K (Figure 5) is in agreement with the C_{2h} symmetry of the structure found in the solid state. Thus, the two sets of resonances at δ 8.12/6.64 and 8.08/7.52 ppm correspond to the two types of 4-Spy ligands in the metallomacrocycle with *exo* and *endo* disposition in the dinuclear rhodium subunit. The olefinic protons of the cod ligands showed five resonances, one of them with double intensity than the others, which were unambiguously identified by means of the ^{1}H-^{1}H COSY spectrum at 218 K (Supporting Information, Figure **S5**). Thus, the expected four resonances for the two olefinic bonds of the cod ligands in the dinuclear subunit were observed at δ 4.80/3.85 and 4.68/4.37 ppm. In addition, the signals at δ 3.93 and 3.85 ppm, that showed no coupling, correspond to the cod ligand of the Rh(cod) units bonded to the pyridine fragments.

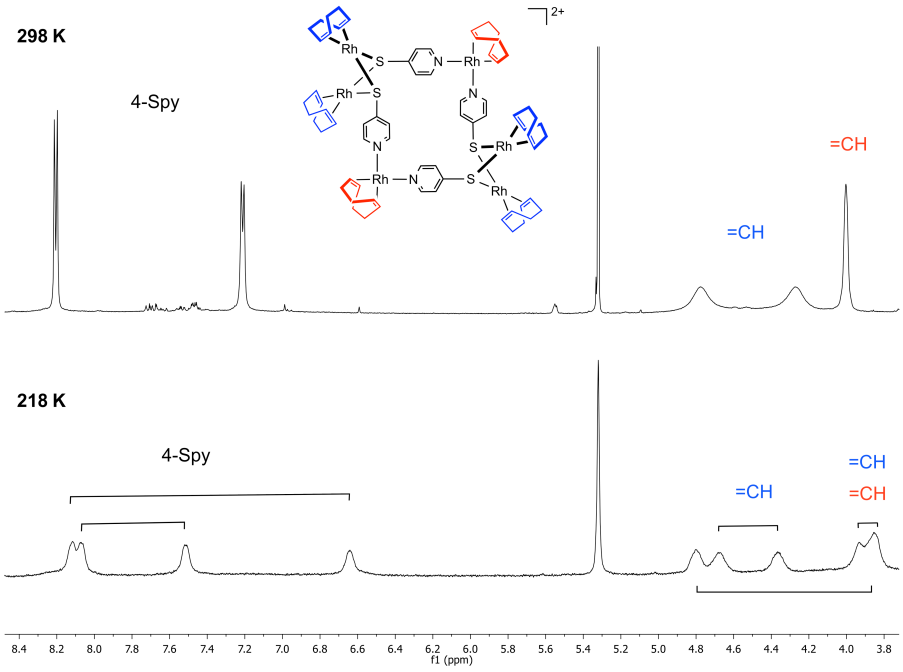

Figure 5. Low field region of ^{1}H NMR spectra (CD_2Cl_2) of metallomacrocycle $(\mathbf{1a})_2$ at 298 K (top) and 218 K (bottom).

In contrast, the spectrum at 298 K (Figure 5) is deceptively simple and shows equivalent 4-Spy ligands and only three resonances (8H each) for the =CH protons of the cod ligands. The ^{1}H-^{1}H NOESY spectrum (Supporting Information, Figure **S6**) was particularly informative because allowed the identification of the =CH resonances of the cod ligand in the dinuclear subunit at δ 4.79 and 4.18 ppm due to observation of proximity cross peaks with the signal at δ 7.20 ppm that corresponds to the β protons of the 4-Spy ligands. In addition, exchange cross-peaks were observed between both =CH resonances, which is indicative that the fluxional process makes equivalent both protons of the same olefinic bond. This process also renders equivalent the olefinic protons of the cod ligands in the Rh(cod) units bonded to pyridine, which were observed at δ 3.97 ppm.

As it has been pointed out above, inversion of the non-planar Rh_2S_2 ring in dinuclear complexes having thiolato ligands as bridges is a common phenomenon that is responsible for their fluxional behavior. In this case, this process would account for the pattern of resonances

observed at room temperature. However, the ring-flipping process not only results in the exchange of the thiolato ligands in *exo* and *endo* disposition but also in the movement of the bulky cod ligands towards the inner part of the metallomacrocycle. Thus, this process requires the concerted motion of the metallomacrocycle in order to allow the rotation about the C-S bonds just for relocating the cod ligands in the outside part of the metallomacrocycle. For that reason, the breaking of the Rh-N bonds in order to assist this process should not be ruled out. Interestingly then, the existence of an equilibrium between the supramolecular species and their corresponding building blocks seems to be responsible for this dynamic behaviour.

The ^{1}H NMR spectrum of compound $[\{Ir_2(\mu\text{-}4\text{-}Spy)_2(cod)_2\}_2\{Ir(cod)\}_2]^{2+}$ (**2b**)$_2$ at room temperature is very similar to that described for the $[Rh_6]$ species, which suggests a similar fluxional behavior for this compound. However, in this case the fluxional process could not be frozen at low temperature precluding further investigation.

The synthesis of metallomacrocycles containing different diolefin ligands, as for example $[\{Rh_2(\mu\text{-}4\text{-}Spy)_2(cod)_2\}_2\{Rh(nbd)\}_2]^{2+}$, was unsuccessful. Thus, even though the reaction of $[Rh(\mu\text{-}4\text{-}Spy)(cod)]_2$ (**1**) with the metal fragment $[Rh(ndb)(NCCH_3)_2]^{+}$ resulted in the formation of $[Rh_6]$ metallomacrocycles, the self-assembly took place in a non selective way because at least four different species were observed in the aromatic region of the ^{1}H NMR spectrum, probably as a consequence of the scrambling of metal fragments having different diolefin ligands (cod and nbd) between the different sites of the metallomacrocyclic framework. In fact, the ESI+ mass spectrum showed, in addition to the species $[Rh_3(Spy)_2(cod)_2(nbd)]^{+}$ at *m/z* 837, the cationic fragment $[Rh_2(SpyH)(Spy)(cod)(nbd)]^{+}$ at *m/z* 627 which support the scrambling process.

Self–assembly reactions involving $[M(\mu\text{-}Spy)(cod)]_2$ (M = Rh (1), Ir (2)) metalloligands and $[M(H_2O)_2(dppp)]^{2+}$ (M = Pd (c), Pt (d)) acceptor units. Interestingly, the attempts for the synthesis of heterometallic metallomacrocycles using *cis*-chelated palladium(II) or

platinum (II) complexes as acceptor building blocks allowed us to obtain of the aimed species. As shown in Scheme 3, treatment of $[M(\mu\text{-4-Spy})(cod)]_2$ (M = Rh(**1**), Ir(**2**)) with the square-planar compounds $[M(H_2O)_2(dppp)](OTf)_2$ (M = Pd (**c**), Pt (**d**)) in 1:1 molar ratio in dichloromethane at room temperature allowed the preparation of a series of hexanuclear $[Rh_4Pd_2]$ $(\mathbf{1c})_2$, $[Rh_4Pt_2]$ $(\mathbf{1d})_2$, $[Ir_4Pd_2]$ $(\mathbf{2c})_2$ and $[Ir_4Pt_2]$ $(\mathbf{2d})_2$ metallocycles that were isolated as yellow-orange solids in good yields.

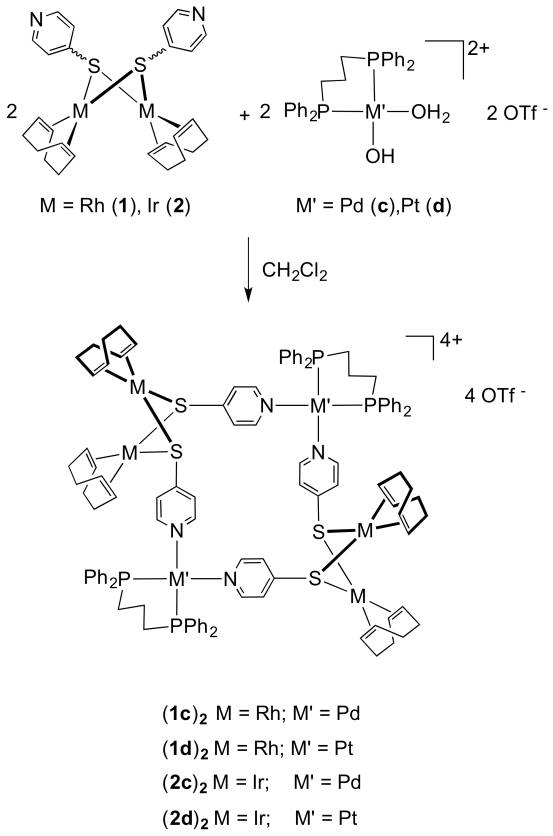

Scheme 3. Self-assembly of hexanuclear $[M_4M'_2]$ metallomacrocycles (M = Rh, Ir; M' = Pd, Pt).

Due to the presence of a diphosphine in the acceptor fragment, monitoring of the reaction solution by $^{31}P\{^1H\}$ NMR spectrometry was very helpful to confirm the formation of the targeted heteronuclear assemblies in all the cases. After reaction completion (*ca*. 2h), the $^{31}P\{^1H\}$ NMR spectra displayed a singlet for both palladium macrocycles ($(\mathbf{1c})_2$ and $(\mathbf{2c})_2$) and

a singlet, with its concomitant satellites, for both platinum species ((**1d**)$_2$ and (**2d**)$_2$). The upfield shift of the ^{31}P signals together with the significant decrease in the value of the $^1J_{P\text{-}Pt}$ coupling constant evidenced the coordination of the pyridine rings to either the palladium or platinum centers.

Analogously to the $[\{M_2(\mu\text{-}4\text{-}Spy)_2(cod)_2\}_2\{M'(cod)\}_2]^{2+}$ (M, M' = Rh, Ir) species described above, the ^{1}H NMR spectra at 298K of the assemblies containing palladium or platinum were deceptively simple. As can be seen in a representative example (compound (**1d**)$_2$ in Figure 6), the spectrum displayed only one signal for the α and β protons of the pyridine groups respectively, and two broad resonances (8H each) for the =CH protons of the cod ligands. The observed pattern is indicative of a fluxional behavior similar to that described for the rhodium and iridium metallomacrocycles. However, in this particular case, the spectra registered in CD_2Cl_2 down to 208K showed a large number of resonances that could not be safely interpreted.

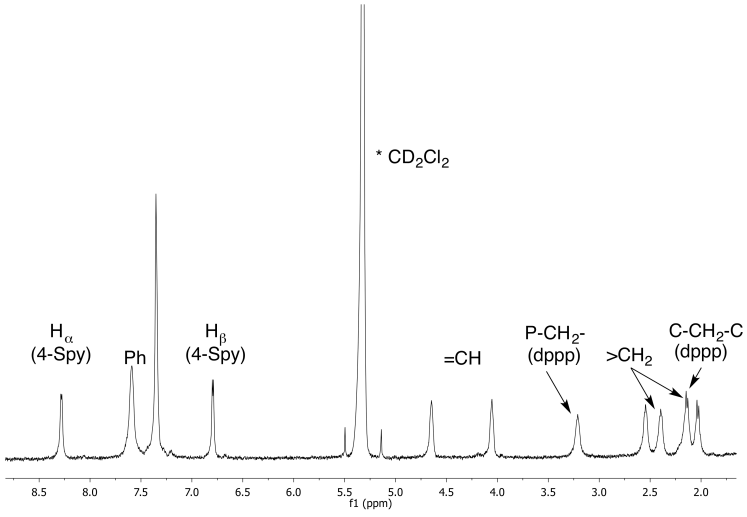

Figure 6. ^{1}H NMR spectrum (298 K, CD_2Cl_2) of metallomacrocycle $[\{Rh_2(\mu\text{-}4\text{-}Spy)_2(cod)]_2\}_2\{Pt(dppp)\}_2](OTf)_4$ (**1d**)$_2$.

The formation of $[\{M_2(\mu\text{-}4\text{-}Spy)_2(cod)]_2\}_2\{M'(dppp)\}_2](OTf)_4$ supramolecules was further supported by high-resolution ESI+ mass spectrometry. The acetone mass spectra of the

compounds showed peaks due to successive loss of triflate anions where, in contrast with the assemblies described above, the hexanuclear metallomacrocycles remain intact. For example, the mass spectrum of compound $[\{Ir_2(\mu\text{-}4\text{-}Spy)_2(cod)]_2\}_2\{Pd(dppp)\}_2](OTf)_4$ $(\mathbf{2c})_\mathbf{2}$ (Figure 7) displays peaks at m/z = 1489.2 and 943.1 that correspond to $[(\mathbf{2c})_\mathbf{2} - 2OTf]^{2+}$ and $[(\mathbf{2c})_\mathbf{2} - 3OTf]^{3+}$, respectively. The doubly charged fragment $[(\mathbf{2c})_\mathbf{2} - 2OTf]^{2+}$ gives rise to the most intense signal in all cases (Supporting Information, Figures **S8-S10**) and no superimposition of smaller species with the same value of m/z was observed after the analysis of the isotope patterns. In addition, it is worthy to point out that the satisfactory mass spectra of the iridium metallomacrocycles $(\mathbf{2c})_\mathbf{2}$ and $(\mathbf{2d})_\mathbf{2}$ confirm the dinuclear formulation of the iridium metalloligand $[Ir(\mu\text{-}4\text{-}Spy)(cod)]_2$ (**2**) whose limited solubility had precluded a complete characterization.

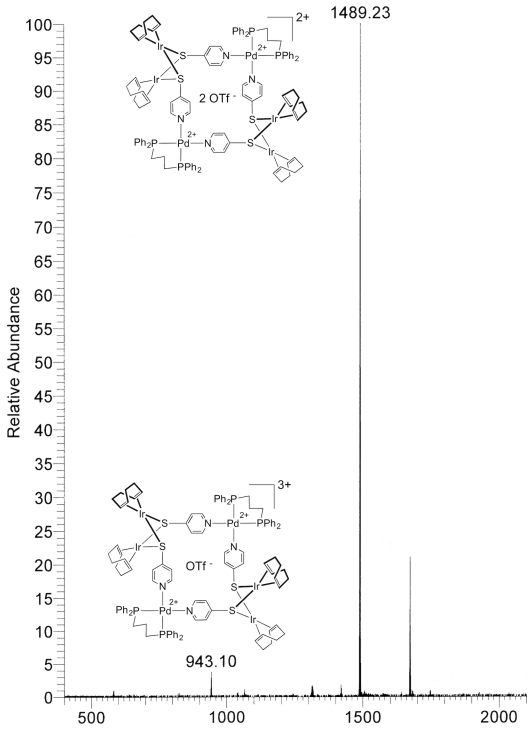

Figure 7. ESI FT-ICR mass spectra of $[\{Ir_2(\mu\text{-}4\text{-}Spy)_2(cod)]_2\}_2\{Pd(dppp)\}_2](OTf)_4$ $(\mathbf{2c})_\mathbf{2}$.

Furthermore, the characterization of these family of compounds was complemented with a X-ray diffraction study on a single crystal of $\mathbf{(1d)_2}$ grown by slow diffusion of diethyl ether

into dichloromethane solution of the compound at 253 K. As featured in Figure 8, the crystal structure shows a macrocyclic square-shaped assembly containing alternating [Rh(μ-4-Spy)(cod)]$_2$ binuclear ligands and Pt(dppp) groups located at the corners of the cationic hexametallic unit. The whole molecule resembles the molecular structure observed for (**1a**)$_2$, where the two "Rh(cod)" corners in (**1a**)$_2$ have been substituted by the "Pt(dppp)" groups (Supporting Information, Figure **S7**). The asymmetric unit of (**1a**)$_2$ contains half of the molecule, that can be expanded *via* the inversion symmetry operation.

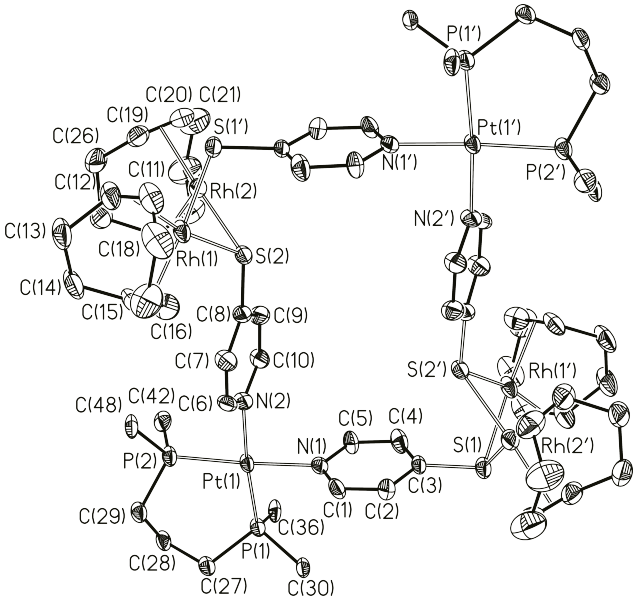

Figure 8. Molecular structure of the cation of (**1d**)$_2$. For clarity only *ipso* carbon atoms of phenyl groups are represented. Primed atoms are related to the non-primed ones through 1-*x*,-*y*,-*z* symmetry operation.

An analysis of the geometrical parameters of the binuclear ligand come out with interatomic bond distances and angles (summarized in Table 3), dihedral angle between mean rhodium coordination planes (74.01(11)º), and interatomic Rh···Rh distance (2.9871(8) Å), very similar to those previously observed in (**1a**)$_2$. This fact pointed out the potential ability of this nonsymmetric bimetallic unit as rigid building block to control self-assembly.

Table 3. Selected bond lengths (Å) and angles (º) for $(\mathbf{1d})_2$.

Rh(1)-S(1')	2.3707(17)	Rh(2)-S(1')	2.3474(16)
Rh(1)-S(2)	2.3781(14)	Rh(2)-S(2)	2.3688(17)
Rh(1)-G(1)	2.018(6)	Rh(2)-G(3)	2.013(7)
Rh(1)-G(2)	2.030(7)	Rh(2)-G(4)	2.027(7)
Pt(1)-P(1)	2.2631(14)	Pt(1)-N(1)	2.088(4)
Pt(1)-P(2)	2.2628(15)	Pt(1)-N(2)	2.109(4)
S(1')-Rh(1)-S(2)	79.52(5)	S(1')-Rh(2)-S(2)	80.18(5)
S(1')-Rh(1)-G(1)	90.9(2)	S(1')-Rh(2)-G(3)	90.1(2)
S(1')-Rh(1)-G(2)	175.8(2)	S(1')-Rh(2)-G(4)	169.7(2)
S(2)-Rh(1)-G(1)	170.3(2)	S(2)-Rh(2)-G(3)	170.2(2)
S(2)-Rh(1)-G(2)	102.3(2)	S(2)-Rh(2)-G(4)	101.7(2)
G(1)-Rh(1)-G(2)	87.3(3)	G(3)-Rh(2)-G(4)	87.5(3)
P(1)-Pt(1)-P(2)	93.22(5)	P(2)-Pt(1)-N(1)	176.82(13)
P(1)-Pt(1)-N(1)	89.46(12)	P(2)-Pt(1)-N(2)	91.92(13)
P(1)-Pt(1)-N(2)	174.85(13)	N(1)-Pt(1)-N(2)	85.40(17)

G(1), G(2), G(3) and G(4) represent the centroid of the C(11)-C(12), C(15)-C(16), C(19)-C(20) and C(23)-C(24) olefinic bonds, respectively.

In fact, coordination of two "Pt(dppp)" fragments through nitrogen atom of 4-Spy moiety gives rise to an heterometallomacrocycle, with alternating Rh_2 and Pt corners. Observed Pt-N bond lengths agree with that reported for the related [(4,4'-bipyridyl)$_4${Pt(dppp)}$_4$](OTf)$_8$,[70] [(dipyridyldibenzotetraaza[14]annulene)$_2${Pt(dppp)}$_2$](OTf)$_4$,[92] [**L1**$_4${Pt(dppp)}$_4$](OTf)$_8$ (**L1** = 2-(3'-(1-methoxycarbonyl-ethylcarbamoyl)-(4,4')-bipyridinyl-3-carbonyl)-amino-propionic acid methyl ester),[83] [(N,N′-bis(3,5-dimethyl-4-pyridinyl)-4-ethoxy-2,6-pyridinedicarboxamide)$_2${Pt(dppp)}$_2$](OTf)$_4$,[93] [**L2**$_2${Pt(dppp)}$_2$](OTf)$_4$ (**L2** = bis(μ_2-3,11-dimethyl-5,13-bis((pyridin-4-yl)-1,9-diazatetracyclo[7.7.1.0^{2,7}.0^{10,15}]heptadeca-2,4,6,10,12,14-hexaene),[94] and [{Pd(η^3-2-Me-C_3H_4)(PPh_2py)$_2$}$_2${Pt(dppp)}$_2$](OTf)$_6$ complexes.[31] The square-planar configuration of platinum atoms is achieved by the coordination of two nitrogen atoms of pyridine-4-thiolate units and the phosphorus atoms of a chelate dppp ligand, with P(1)-Pt(1)-N(2) and P(2)-Pt(1)-N(2) angles (89.46(12) and 91.92(13)º, respectively) very close to the ideal 90º *cis* angle values. Substitution of cod by dppp seems to hardly affect to the macrocyclic core dimensions that are 6.6354(16) x 9.6200(15) Å for this compound.

On the other hand, the bite angle of the bidentate chelate dppp is close to those reported in the literature for M(dppp) fragments. The 6-membered Pt-P(1)-C(27)-C(28)-C(29)-P(2) metallocycle adopts a $^1C_4$ chair conformation (Q = 0.640(5) Å, Θ = 13.8(4)º and ϕ = -173(2)º).[95] Within this arrangement, π···π interactions are observed between equatorial phenyl rings of the diphosphine and the pyridine rings (Figure 9 and Table **S1** in Supporting Information).

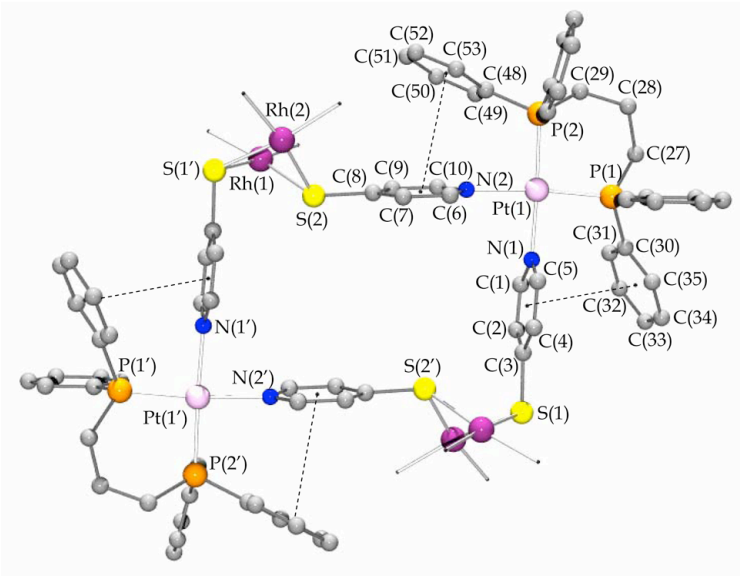

Figure 9. Schematic representation of the π··· π interactions in $(\mathbf{1d})_2$. For clarity carbon atoms of cod fragments have been omitted. Primed atoms are related to the non-primed ones through 1-*x*,-*y*,-*z* symmetry operation.

Packing arrangement of $(\mathbf{1d})_2$ is very different than that observed in $(\mathbf{1a})_2$, as it shows columnar stacking along *a* axis with perfect overlay of the metallomacrocycles (Figure 10).

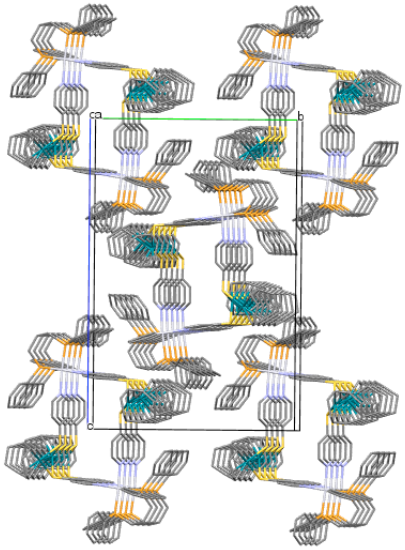

Figure 10. Packing diagram for $(\mathbf{1d})_2$. For simplicity, hydrogen atoms, counterions and solvent molecules have been omitted.

Self-assembly reactions involving [Rh(μ-4-Spy)(nbd)]$_2$ (3) and [Rh(μ-4-Spy)(CO)(PPh$_3$)]$_2$ (4). In contrast with [Rh(μ-4-Spy)(cod)]$_2$, the dinuclear compound [Rh(μ-4-Spy)(nbd)]$_2$ (**3**) was not an effective building block. Monitoring of the reaction of **3** with [Rh(nbd)(NCCH$_3$)$_2$]$^+$ in CD_2Cl_2 evidenced the formation of the metallomacrocycle [{Rh$_2$(μ-4-Spy)$_2$(nbd)$_2$}$_2${Rh(nbd)}$_2$]$^{2+}$ which was identified by the set of characteristic resonances for the α and β protons of the pyridine-4-thiolato ligands: four doublets at δ 8.22, 8.18, 7.08 and 6.90 ppm ($^1J_{H\text{-}H} \approx 6$ Hz). However, we could not isolate a well-defined product in the solid state and, after several attempts, we only were able to obtain orange solids with poor defined NMR spectra. Most probably, this fact could be a consequence of the lability of the formed assembly, which is in agreement with the stronger π–acceptor character of the 2,5-norbornadiene ligands compared to 1,5-cyclooctadiene, which in turn reduces the electronic density on the peripheral nitrogen donor atoms, thereby decreasing their coordinating ability.

A potential catalytic application of the diolefin-based metallomacrocycles is the olefin hydroformylation.[47,96] However, under syngas (H_2/CO) pressure and an excess of phosphine ligand the diolefin rhodium catalyst precursors readily transform into the corresponding CO/PPh$_3$ derivatives. In order to explore the stability of the metallocycles based on "Rh(CO)(PPh$_3$)" metal fragments, self-assembly reactions involving the metalloligand [Rh(μ-4-Spy)(CO)(PPh$_3$)]$_2$ (**4**) have been carried out. Reaction of (**4**) with [Rh(cod)(NCCH$_3$)$_2$]BF$_4$ (**a**) in a 1:1 molar ratio in CH_2Cl_2 gave an orange-brown crude product that was isolated after the addition of diethyl ether. Interestingly, in contrast to that observed for the previously described metallomacrocycles, the NMR spectra of this material indicated the presence of a mixture of self-assembled species with a clear predominance of one of them. So, the ^{1}H NMR spectrum (Supporting Information, Figure **S11**) showed four intense sharp doublets that indicated the equivalence of pyridines into pairs while ^{31}P{^{1}H} NMR spectrum (Supporting Information, Figure **S12**) displayed as the most intense resonance a doublet ($^1J_{P\text{-}Rh}$ = 129 Hz)

that is in accordance with the equivalence of the four phosphorus nuclei. In addition, the ^{1}H-^{1}H NOESY spectrum showed proximity cross peaks between one of the β pyridine protons and a phenyl group of triphenylphosphine. Since the metalloligand **4** can adopt different structures depending on the relative disposition of the PPh_3 and CO ligands, four different isomeric metallocycles can be envisaged *i.e*. two *cis-cis* (C_{2h} and C_s symmetry) and two *trans-trans* (C_1 and C_2 symmetry). NMR data strongly suggest that the major species from the **4** + **a** self-assembly should be the *cis-cis* isomer of C_{2h} symmetry (represented in Figure 11), which reinforce the proposed *cis* disposition of the PPh_3/CO ligands in compound [Rh(μ-4-Spy)(CO)(PPh_3)]$_2$ (**4**).

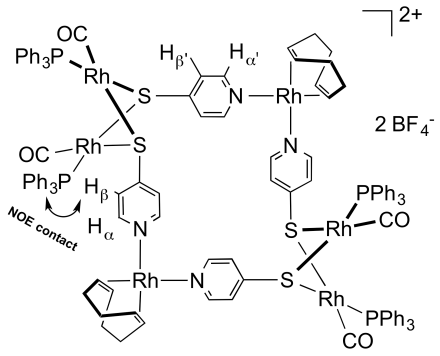

Figure 11. Proposed structure of the predominant species from the self-assembly of [Rh(μ-4-Spy)(CO)(PPh_3)]$_2$ (**4**) and [Rh(cod)($NCCH_3$)$_2$]BF_4 (**a**).

Conclusions

The dinuclear complexes [M(4-Spy)(cod)]$_2$ (M = Rh, Ir) supported by pyridine-4-thiolato bridged ligands have been proved to be effective ditopic building blocks for the construction of new supramolecular architectures. The two nucleophilic nitrogen atoms of the terminal pyridine groups allow these compounds to self-assemble with suitable acceptor metallic fragments [M(cod)($NCCH_3$)$_2$]$^+$ (M = Rh, Ir) or [M(H_2O)$_2$(dppp)](OTf)$_2$ (M = Pd, Pt) yielding

homo- and hetero- hexanuclear metallomacrocycles of composition $[Rh_4M_2]$ and $[Ir_4M_2]$. This supramolecular species are composed of alternating dinuclear (Rh_2 or Ir_2) and mononuclear corners (Rh, Ir, Pd, and Pt) supported by four pyridine-4-thiolate linkers resulting in rectangular assemblies with cavities of 9.6 x 6.6 Å.

Although multinuclear NMR spectroscopy is indicative of a *syn* disposition of the pyridine-4-thiolate fragments in the free dinuclear metalloligands, the *anti* conformation adopted by these compounds when forming the metallocycles, implies a process of sulfur inversion associated with the self-assembly reactions. In addition, all the obtained macrocycles are stereochemically non-rigid in solution. The study of this behavior by ^1H NMR spectroscopy revealed the existence of a dynamic equilibrium between the supramolecular species and their corresponding building blocks.

The related dinuclear complex $[Rh(4\text{-}Spy)(nbd)]_2$ and $[Rh(4\text{-}Spy)(CO)(PPh_3)]_2$ did not self-assemble as effectively as $[M(4\text{-}Spy)(cod)]_2$ (M = Rh, Ir). The metallomacrocycles involving $[Rh(4\text{-}Spy)(nbd)]_2$ were found to be labile, which precluded their isolation from the reaction solution. This fact could be related with the stronger π-acceptor character of ndb compared to cod, which reduces the coordination ability to the pyridine fragments. On the other hand, the complex $[Rh(4\text{-}Spy)(CO)(PPh_3)]_2$ gave a mixture of supramolecules derived from the relative disposition of the CO and PPh_3 ligands at the rhodium centers.

Finally, the introduction of Rh(cod) functionality in these supramolecules opens the possibility of undergoing future studies of their catalytic activity in several processes.

Supporting Information Available: X-ray crystallographic files in CIF format for the structure determination of metallomacrocycles $(\mathbf{1a})_2$ and $(\mathbf{1d})_2$. NMR spectra of $(\mathbf{1a})_2$ **and** $(\mathbf{4a})_2$, ESI-MS spectra of $(\mathbf{1c})_2$, $(\mathbf{1d})_2$ and $(\mathbf{2d})_2$ and geometrical parameters of the π··· π interactions in $(\mathbf{1d})_2$. This material is available free of charge via the Internet at http://pubs.acs.org.

Corresponding Author.

E-mail: montse.ferrer@qi.ub.es, perez@unizar.es

Acknowledgments

Financial support for this work was provided by the Ministerio de Economía y Competitividad (MINECO/FEDER) of Spain (Projects CTQ2010-15221 and CTQ2012-31335), Diputación General de Aragón (Group E07) and Fondo Social Europeo.

References

(1) Leininger, S.; Olenyuk, B.; Stang, P. J. *Chem. Rev.* **2000**, *100*, 853-907.

(2) Swiegers, G. F.; Malefetse, T. J. *Chem. Rev.* **2000**, *100*, 3483-3537.

(3) Cotton, F. A.; Lin, C.; Murillo, C. A. *Acc. Chem. Res.* **2001**, *34*, 759-771.

(4) Cronin, L. *Annu. Rep. Prog. Chem., Sect. A, Inorg. Chem.* **2004**, *100*, 323-383.

(5) Wurthner, F.; You, C. C.; Saha-Moller, C. R. *Chem. Soc. Rev.* **2004**, *33*, 133-146.

(6) Amijs, C. H. M.; van Klink, G. P. M.; van Koten, G. *Dalton Trans.* **2006**, 308-327.

(7) Chen, C. L.; Zhang, J. Y.; Su, C. Y. *Eur. J. Inorg. Chem.* **2007**, 2997-3010.

(8) Nitschke, J. R. *Acc. Chem. Res.* **2007**, *40*, 103-112.

(9) Kumar, A.; Sun, S. S.; Lees, A. J. *Coord. Chem. Rev.* **2008**, *252*, 922-939.

(10) Northrop, B. H.; Yang, H. B.; Stang, P. J. *Chem. Commun.* **2008**, 5896-5908.

(11) Northrop, B. H.; Zheng, Y. R.; Chi, K. W.; Stang, P. J. *Acc. Chem. Res.* **2009**, *42*, 1554-1563.

(12) Chakrabarty, R.; Mukherjee, P. S.; Stang, P. J. *Chem. Rev.* **2011**, *111*, 6810-6918.

(13) Amouri, H.; Desmarets, C.; Moussa, J. *Chem. Rev.* **2012**, *112*, 2015-2041.

(14) Cook, T. R.; Zheng, Y. R.; Stang, P. J. *Chem. Rev.* **2013**, *113*, 734-777.

(15) Pariya, C.; Sparrow, C. R.; Back, C. K.; Sandi, G.; Fronczek, F. R.; Maverick, A. W. *Angew. Chem. Int. Ed.* **2007**, *46*, 6305-6308.

(16) Chatterjee, B.; Noveron, J. C.; Resendiz, M. J. E.; Liu, J.; Yamamoto, T.; Parker, D.; Cinke, M.; Nguyen, C. V.; Arif, A. M.; Stang, P. J. *J. Am. Chem. Soc.* **2004**, *126*, 10645-10656.

(17) Yoshizawa, M.; Klosterman, J. K.; Fujita, M. *Angew. Chem. Int. Ed.* **2009**, *48*, 3418-3438.

(18) Lee, S. J.; Lin, W. B. *Acc. Chem. Res.* **2008**, *41*, 521-537.

(19) Zhang, Q. A.; He, L. S.; Liu, J. M.; Wang, W.; Zhang, J. Y.; Su, C. Y. *Dalton Trans*. **2010**, *39*, 11171-11179.

(20) Milde, B.; Packheiser, R.; Hildebrandt, S.; Schaarschmidt, D.; Ruffer, T.; Lang, H. *Organometallics* **2012**, *31*, 3661-3671.

(21) Schelter, E. J.; Prosvirin, A. V.; Dunbar, K. R. *J. Am. Chem. Soc.* **2004**, *126*, 15004-15005.

(22) Karadas, F.; Schelter, E. J.; Prosvirin, A. V.; Bacsa, J.; Dunbar, K. R. *Chem. Commun.* **2005**, 1414-1416.

(23) Ono, K.; Yoshizawa, M.; Tatsuhisa, K. C.; Fujita, M. *Chem. Commun.* **2008**, 2328-2330.

(24) Han, F. S.; Higuchi, M.; Kurth, D. G. *J. Am. Chem. Soc.* **2008**, *130*, 2073-2081.

(25) Sun, Q. F.; Wong, K. M. C.; Liu, L. X.; Huang, H. P.; Yu, S. Y.; Yam, V. W. W.; Li, Y. Z.; Pan, Y. J.; Yu, K. C. *Inorg. Chem.* **2008**, *47*, 2142-2154.

(26) Yamamoto, Y.; Tamaki, Y.; Yui, T.; Koike, K.; Ishitani, O. *J. Am. Chem. Soc.* **2010**, *132*, 11743-11752.

(27) Steed, J. W. *Chem. Soc. Rev.* **2009**, *38*, 506-519.

(28) Gao, J.; Riis-Johannessen, T.; Scopelliti, R.; Qian, X. H.; Severin, K. *Dalton Trans*. **2010**, *39*, 7114-7118.

(29) Yao, L. Y.; Qin, L.; Xie, T. Z.; Li, Y. Z.; Yu, S. Y. *Inorg. Chem.* **2011**, *50*, 6055-6062.

(30) Alvarez-Vergara, M. C.; Casado, M. A.; Martin, M. L.; Lahoz, F. J.; Oro, L. A.; Perez-Torrente, J. J. *Organometallics* **2005**, *24*, 5929-5936.

(31) Angurell, I.; Ferrer, M.; Gutierrez, A.; Martinez, M.; Rodriguez, L.; Rossell, O.; Engeser, M. *Chem.-Eur. J.* **2010**, *16*, 13960-13964.

(32) Ferrer, M.; Gutierrez, A.; Rodriguez, L.; Rossell, O.; Ruiz, E.; Engeser, M.; Lorenz, Y.; Schilling, R.; Gomez-Sal, P.; Martin, A. *Organometallics* **2012**, *31*, 1533-1545.

(33) Zanardi, A.; Mata, J. A.; Peris, E. *J. Am. Chem. Soc.* **2009**, *131*, 14531-14537.

(34) Suijkerbuijk, B. M. J. M.; Schamhart, D. J.; Kooijman, H.; Spek, A. L.; van Koten, G.; Gebbink, R. J. M. K. *Dalton Trans*. **2010**, *39*, 6198-6216.

(35) Park, J.; Hong, S. *Chem. Soc. Rev*. **2012**, *41*, 6931-6943.

(36) Bera, J. K.; Smucker, B. W.; Walton, R. A.; Dunbar, K. R. *Chem. Commun*. **2001**, 2562-2563.

(37) Bera, J. K.; Bacsa, J.; Smucker, B. W.; Dunbar, K. R. *Eur. J. Inorg. Chem*. **2004**, 368-375.

(38) Kuang, S. M.; Fanwick, P. E.; Walton, R. A. *Inorg. Chem*. **2002**, *41*, 1036-1038.

(39) Song, L. C.; Jin, G. X.; Zhang, W. X.; Hu, Q. M. *Organometallics* **2005**, *24*, 700-706.

(40) Cotton, F. A.; Jin, J. Y.; Li, Z.; Liu, C. Y.; Murillo, C. A. *Dalton Trans*. **2007**, 2328-2335.

(41) Zhao, L.; Ghosh, K.; Zheng, Y.; Lyndon, M. M.; Williams, T. I.; Stang, P. J. *Inorg. Chem*. **2009**, *48*, 5590-5592.

(42) Ara, I.; Chaouche, N.; Fornies, J.; Fortuno, C.; Kribii, A.; Martin, A. *Eur. J. Inorg. Chem*. **2005**, 3894-3901.

(43) Ciriano, M. A.; Perez-Torrente, J. J.; Lahoz, F. J.; Oro, L. A. *J. Chem. Soc., Dalton Trans*. **1992**, 1831-1837.

(44) Casado, M. A.; Perez-Torrente, J. J.; Lopez, J. A.; Ciriano, M. A.; Lahoz, F. J.; Oro, L. A. *Inorg. Chem*. **1999**, *38*, 2482-2488.

(45) Miranda-Soto, V.; Perez-Torrente, J. J.; Oro, L. A.; Lahoz, F. J.; Martin, M. L.; Parra-Hake, M.; Grotjahn, D. B. *Organometallics* **2006**, *25*, 4374-4390.

(46) Hernandez-Gruel, M. A. F.; Gracia-Arruego, G.; Rivas, A. B.; Dobrinovitch, I. T.; Lahoz, F. J.; Pardey, A. J.; Oro, L. A.; Perez-Torrente, J. J. *Eur. J. Inorg. Chem*. **2007**, 5677-5683.

(47) Rivas, A. B.; Gascon, J.; Lahoz, F. J.; Balana, A. I.; Pardey, A. J.; Oro, L. A.; Perez-Torrente, J. J. *Inorg. Chem.* **2008**, *47*, 6090-6104.

(48) Perez-Torrente, J. J.; Jimenez, M. V.; Hernandez-Gruel, M. A. E.; Fabra, M. J.; Lahoz, F. J.; Oro, L. A. *Chem.-Eur. J.* **2009**, *15*, 12212-12222.

(49) Aullon, G.; Ujaque, G.; Lledos, A.; Alvarez, S. *Chem.-Eur. J.* **1999**, *5*, 1391-1410.

(50) Capdevila, M.; Gonzalez-Duarte, P.; Foces-Foces, C.; Cano, F. H.; Martinez-Ripoll, M. *J. Chem. Soc., Dalton Trans.* **1990**, 143-149.

(51) Rivera, G.; Bernes, S.; de Barbarin, C.; Torrens, H. *Inorg. Chem.* **2001**, *40*, 5575-5580.

(52) Oster, S. S.; Jones, W. D. *Inorg. Chim. Acta* **2004**, *357*, 1836-1846.

(53) Chikamoto, Y.; Kawamoto, T.; Igashira-Kamiyama, A.; Konno, T. *Inorg. Chem.* **2005**, *44*, 1601-1610.

(54) Chong, S. H.; Koh, L. L.; Henderson, W.; Hor, T. S. A. *Chem.- Asian J.* **2006**, *1*, 264-272.

(55) Boudreau, J.; Grenier-Desbiens, J.; Fontaine, F. G. *Eur. J. Inorg. Chem.* **2010**, 2158-2164.

(56) Ruiz, N.; Castillon, S.; Ruiz, A.; Claver, C.; Aaliti, A.; Alvarez-Larena, A.; Piniella, J. F.; Germain, G. *J. Chem. Soc., Dalton Trans.* **1996**, 969-973.

(57) Castellanos-Paez, A.; Thayaparan, J.; Castillon, S.; Claver, C. *J. Organomet. Chem.* **1998**, *551*, 375-381.

(58) Bayon, J. C.; Claver, C.; Masdeu-Bulto, A. M. *Coord. Chem. Rev.* **1999**, *193-5*, 73-145.

(59) Pamies, O.; Net, G.; Ruiz, A.; Bo, C.; Poblet, J. M.; Claver, C. *J. Organomet. Chem.* **1999**, *586*, 125-137.

(60) Freixa, Z.; Martin, E.; Gladiali, S.; Bayon, J. C. *Appl. Organomet. Chem* **2000**, *14*, 57-65.

(61) Han, Y. F.; Lin, Y. J.; Jia, W. G.; Jin, G. X. *Dalton Trans.* **2009**, 2077-2080.

(62) Wang, H.; Guo, X. Q.; Zhong, R.; Lin, Y. J.; Zhang, P. C.; Hou, X. F. *J. Organomet. Chem.* **2009**, *694*, 3362-3368.

(63) Wang, H.; Zhong, R.; Guo, X. Q.; Feng, X. Y.; Hou, X. F. *Eur. J. Inorg. Chem.* **2010**, 174-178.

(64) Tzeng, B. C.; Ding, C. S.; Chang, T. Y.; Hu, C. C.; Lee, G. H. *CrystEngComm.* **2012**, *14*, 8228-8235.

(65) Giordano, G.; Crabtree, R. H. *Inorg. Synth.* **1979**, *19*, 218-220.

(66) Abel, E. W.; Bennett, M. A.; Wilkinson, G. *J. Chem. Soc.* **1959**, 3178-3182.

(67) Herde, J. L.; Lambert, J. C.; Senoff, C. V. *Inorg. Synth.* **1971**, *15*, 18-20.

(68) Uson, R.; Oro, L. A.; Cabeza, J. A.; Bryndza, H. E.; Stepro, M. P. *Inorg. Synth.* **1985**, *23*, 126-127.

(69) Jegorov, A.; Podlaha, J.; Podlahova, J.; Turecek, F. *J. Chem. Soc., Dalton Trans.* **1990**, 3259-3263.

(70) Stang, P. J.; Cao, D. H.; Saito, S.; Arif, A. M. *J. Am. Chem. Soc.* **1995**, *117*, 6273-6283.

(71) Green, M.; Kuc, T. A.; Taylor, S. H. *J. Chem. Soc. A* **1971**, 2334-2335.

(72) *SAINT+, Version 6.01: Area Detector Integration Software, Bruker AXS*, Madison, WI, 2001.

(73) *SADABS, Area Detector Absorption Correction Program, Bruker AXS*, Madison, WI, 1996.

(74) Sheldrick, G. M. *Acta Crystallogr.* **1990**, *A46*, 467-473.

(75) Sheldrick, G. M. *Methods Enzymol.* **1997**, *276*, 628-641.

(76) Sheldrick, G. M. *Acta Crystallogr.* **2008**, *A64*, 112-122.

(77) Nardelli, M. *Comput. Chem.* **1983**, *7*, 95-98.

(78) Nardelli, M. *J. Appl. Crystallogr.* **1995**, *28*, 659-673.

(79) Cotton, F. A.; Lin, C.; Murillo, C. A. *Inorg. Chem.* **2001**, *40*, 478-484.

(80) Teo, P.; Koh, L. L.; Hor, T. S. A. *Inorg. Chem.* **2008**, *47*, 6464-6474.

(81) Granzhan, A.; Riis-Johannessen, T.; Scopelliti, R.; Severin, K. *Angew. Chem. Int. Ed.* **2010**, *49*, 5515-5518.

(82) Wang, X. B.; Huang, J.; Xiang, S. L.; Liu, Y.; Zhang, J. Y.; Eichhofer, A.; Fenske, D.; Bai, S.; Su, C. Y. *Chem. Commun.* **2011**, *47*, 3849-3851.

(83) Rang, A.; Nieger, M.; Engeser, M.; Lutzen, A.; Schalley, C. A. *Chem. Commun.* **2008**, 4789-4791.

(84) Vandersluis, P.; Spek, A. L. *Acta Crystallogr.* **1990**, *A46*, 194-201.

(85) Abel, E. W.; Bhargava, S. K.; Orrell, K. G. *Prog. Inorg. Chem.* **1984**, *32*, 1-118.

(86) Brunner, H.; Bugler, J.; Nuber, B. *Tetrahedron: Asymmetry* **1996**, *7*, 3095-3098.

(87) Fernandez, E.; Ruiz, A.; Castillon, S.; Claver, C.; Piniella, J. F.; Alvarez-Larena, A.; Germain, G. *J. Chem. Soc., Dalton Trans.* **1995**, 2137-2142.

(88) Fandos, R.; Martinez-Ripoll, M.; Otero, A.; Ruiz, M. J.; Rodriguez, A.; Terreros, P. *Organometallics* **1998**, *17*, 1465-1470.

(89) Wark, T. A.; Stephan, D. W. *Can. J. Chem.* **1990**, *68*, 565-569.

(90) Jones, W. D.; Garcia, J.; Torrens, H. *Acta Crystallogr.* **2005**, *E61*, M2204-M2206.

(91) Delferro, M.; Cauzzi, D.; Pattacini, R.; Tegoni, M.; Graiff, C.; Tiripicchio, A. *Eur. J. Inorg. Chem.* **2008**, 2302-2312.

(92) Beves, J. E.; Chapman, B. E.; Kuchel, P. W.; Lindoy, L. F.; McMurtrie, J.; McPartlin, M.; Thordarson, P.; Wei, G. *Dalton Trans.* **2006**, 744-750.

(93) Capo, M.; Benet-Buchholz, J.; Ballester, P. *Inorg. Chem.* **2008**, *47*, 10190-10192.

(94) Weilandt, T.; Kiehne, U.; Bunzen, J.; Schnakenburg, G.; Lutzen, A. *Chem.-Eur. J.* **2010**, *16*, 2418-2426.

(95) Cremer, D.; Pople, J. A. *J. Am. Chem. Soc.* **1975**, *97*, 1354-1358.

(96) Leighton, J. L. *Modern Rhodium-Catalyzed Organic Reactions*. Wiley-VCH: Weinheim, 2005.

Table of contents

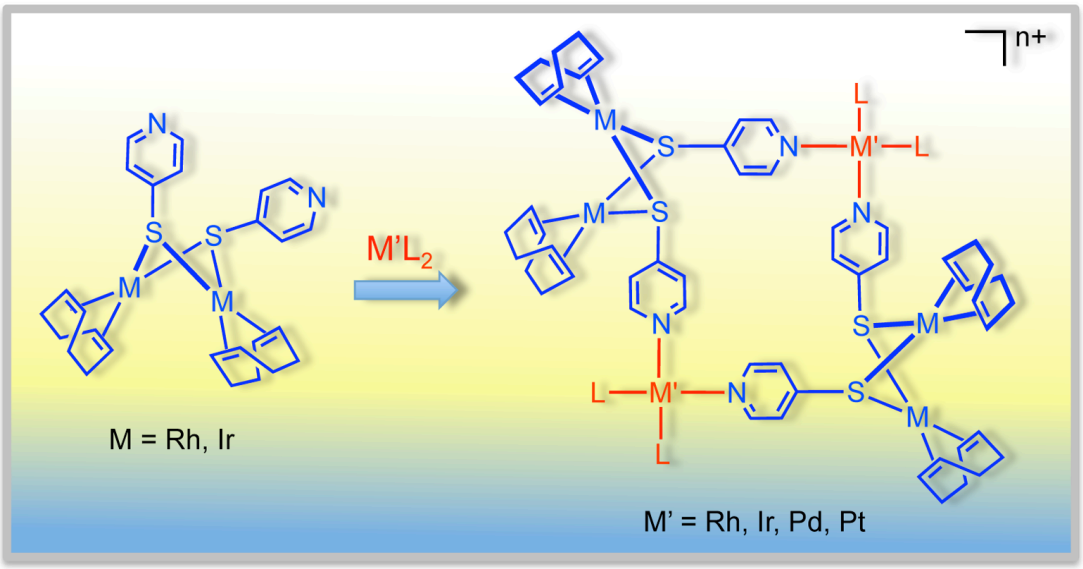

Synopsis

A series of new dinuclear pyridine-4-thiolato compounds $[M(\mu\text{-}4\text{-}Spy)(diolef)]_2$ (M = Rh, Ir) have been used as ditopic building blocks for the construction of homo and heterometallic rectangular assemblies composed of alternating dinuclear (Rh_2 or Ir_2) and mononuclear corners (Rh, Ir, Pd, and Pt) supported by four pyridine-4-thiolate linkers. These metallocycles are stereochemically non-rigid in solution and their fluxional behavior has been studied by variable temperature NMR spectroscopy.